IOWA STATE UNIVERSITY
Digital Repository

1986

Analysis of a GPS aided inertial navigation system using the delayed state Kalman filter

Paul William McBurney
Iowa State University

Follow this and additional works at: https://lib.dr.iastate.edu/rtd

Part of the Computer Engineering Commons, and the Electrical and Computer Engineering Commons

Recommended Citation

www.manaraa.com

Analysis of a GPS aided inertial navigation system

using the delayed state Kalman filter

by

Paul William McBurney

A Thesis Submitted to the

Graduate Faculty in Partial Fulfillment of the

Requirements for the Degree of

MASTER OF SCIENCE

Department: Electrical Engineering and
Computer Engineering
Major: Electrical Engineering

Iowa State University
Ames, Iowa

1986

TABLE OF CONTENTS

I. INTRODUCTION

A. Review of Aided Inertial Navigation Systems

A stand-alone inertial navigation system (INS) uses gyroscopes for inertial stabilization and accelerometers to measure vehicle position and velocity with respect to a given reference. Because the gyroscopes tend to drift out of calibration, the accuracy of the system degrades with increasing time from reset. Aided navigation systems have been developed to provide an accurate reference so that the INS errors can be estimated. When the errors are found, an improved estimate of position and velocity can be obtained. The error estimates may also be used to reset the gyros after some specified time interval to keep the errors small.

Many types of aiding sources and system structures have been developed since the early 1940s. These include airborne systems which receive aiding measurements from ground stations (LORAN) as well as marine-based systems which obtain aiding information from satellites (NAV-SAT). The Global Positioning System (GPS), a satellite network which is currently partially in place although not in full deployment, promises to be an excellent aiding source. GPS alone can provide discrete estimates of a user's position, velocity, and time with respect to a specified coordinate frame and time reference. When the system is fully operational, at least four satellites will be "visible" on a nearly twenty-four hour basis anywhere on the near-earth. GPS aided inertial navigation systems are already available to civilian users.

They have been used with such success that they are called Highly Accurate Inertial Navigation Systems (HAINS) [1].

In a typical feedforward complementary-type aided INS (see Figure 2), a measured quantity from an aiding source is compared with the corresponding quantity computed using the inertial system's current position and/or velocity [2]. The difference is then related to the INS position and/or velocity errors and the aiding source errors. The best estimates of INS position and velocity are obtained by first using the difference quantity to estimate the INS errors and then subtracting the errors from the INS estimates. An estimator is needed to separate out the INS and aiding source errors. The estimator does not operate on the total position and velocity quantities. They pass through the system until the estimated errors are subtracted out.

The task of estimating the INS errors is complicated by several factors. There are usually several measurements available which are related to the same quantities so that each measurement must be given its proper weight depending on the confidence in the measurement. There is also a considerable amount of measurement noise associated with the aiding source measurement. The gyro errors will be random in nature. It is clear that an optimal estimator is needed to process the difference measurements and extract the best estimate of INS errors.

The Kalman filter has proven to be the answer to the estimation problem. The error quantities become the state vector of the filter which is the random process to be estimated. To implement the Kalman filter, the dynamic properties of the state vector are modelled by

defining the process state equation, the input is modelled with the measurement equation, and the covariance structure of the noise in the process and measurement equations are defined. It is then a routine matter to obtain a set of recursive equations which will yield an optimal estimate of the current state of the random process based on a set of noisy measurements which are related to the current state.

When GPS is used as an aiding source, there are generally eight measurements available within a certain time interval (two measurements from each of four satellites). These are the pseudo-range and range rate (also known as the delta-range) of the magnitude of the distance from the GPS receiver to the satellite. Since the satellite position is considered given, it is possible to calculate what the measurement should be using the INS current position and the given satellite position. This assumes, of course, that the positions can be brought into the same coordinate frame. The difference of the computed and measured quantities becomes the observable to the Kalman filter and will be the difference of the INS errors and the aiding source errors since the true values subtract out.

The range rate measurement is actually the change of the GPS carrier phase over a specified small interval of time. This time interval is known as the delta-range integration interval. The range rate is proportional to the Doppler shift of the GPS carrier due to the relative motion between the receiver and the satellite. It is not physically possible to measure instantaneous frequency. It is safe to say that the real measurement is the average (integral) of the range rate over the

integration interval. Some aided inertial systems consider the measurement to be a point measure of the range rate. Using this model, when the computed and measured range rate are compared the difference will be proportional to the INS velocity errors and the GPS clock fractional frequency error. However, to assume that instantaneous velocity measurements are observable is very optimistic and quite risky. But, this type of measurement model might be a fair approximation if the integration interval and the vehicle accelerations are very small.

If the measurement equation is considered to be the integral of the computed Doppler shift less the measured Doppler shift over the time interval, the measurement can be shown to be proportional to the difference of the ranges evaluated at the endpoints of the interval and to the difference of the GPS clock offset errors at the endpoints of the interval. This is a much safer model because there is no problem assuming instantaneous position measurements can be obtained.

The only problem with this measurement model is that it does not fit the form of the usual Kalman filter measurement equation. The observable is related to the present as well as the past filter state. This problem can be alleviated by using the delayed state Kalman filter which has a measurement equation that allows for the current measurement to be proportional to the current and previous state vectors. This filter will then allow for optimal processing of the delta-range measurements. This problem can also be seen as just a two point smoothing problem. If desired, the delayed state Kalman filter could be generalized to include more states [3].

B. GPS Summary

A brief summary of GPS and of the process used to detect and decode the satellite signals is helpful in describing the contribution GPS provides as an aiding source to an INS. When the system is fully operational, there will be eighteen satellites: three in each of six rings (plus three active spares) in non-synchronous orbits with one-half day periods (see Figure 1). Their orbits are spaced so that at least four satellites will be observable at any time. Each satellite transmits two codes: the precision code which offers high precision but is reserved for military purposes, and the coarse/acquisition code (C/A code) which is available for civilian use [8, 9]. (Use of the C/A code will be assumed here although the P code would be used in much the same way.)
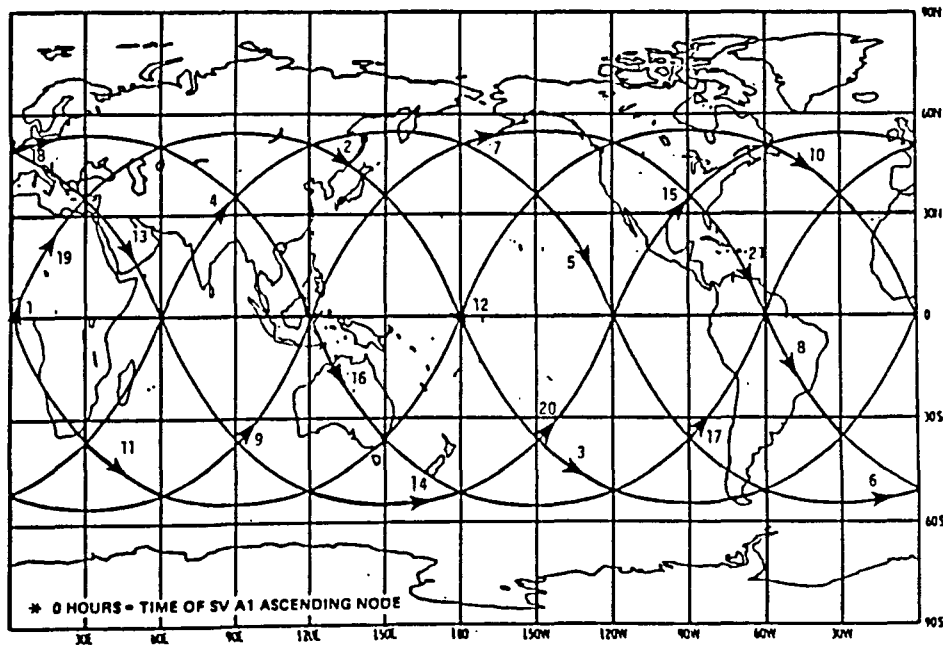

Figure 1. GPS satellite configuration

The phase of the GPS carrier as well as the information modulated onto the carrier is used in obtaining a navigation solution. Each satellite has a unique pseudo-random binary (+1, -1) sequence which modulates the phase of the carrier signal. A GPS receiver has each of the pseudo-random sequences as well as an almanac of the current satellite constellation stored in memory. For a given GPS time and position, the GPS receiver can determine which satellites will be available, and of those, which will be in the best configuration to minimize Geometric Dilution of Precision (GDOP) [8, 9]. For each of the chosen satellites, the receiver generates the pseudo-random sequence and computes the cross-correlation between the locally generated code and the received code. The receiver then shifts the locally generated code to match the incoming code, and thus it measures range plus clock offset in this manner. The received signal will also be out of phase with the locally generated signal because of the signal propagation time and also because of the Doppler shift due to the relative motion between the satellite and the receiver. The receiver has to shift the phase of the locally generated signal to achieve maximum correlation between the received and local signal. If acceptable locking is achieved, the receiver can then decode the satellite message. This operation is performed with a Costas type phase lock loop. This message contains the timing and satellite position data (plus many other blocks of data) needed when solving for receiver position, velocity and time.

The code difference measurement is proportional to the signal propagation time and is used to find the pseudo-range from the receiver

to the satellite. This distance measurement is called a pseudo-range because it contains the effects of receiver and satellite clock errors as well as the desired propagation delay. The delta-range or range rate measurement is obtained by taking the difference of the predicted and measured phase shifts over some specified time interval and then dividing this by the time interval [6]. The pseudo-range, the delta-range, and the decoded satellite message from each of the four satellites are the contributions that GPS makes as the aiding source in an aided INS.

The receiver clock offset and fractional frequency (the actual frequency offset divided by nominal frequency) errors are mainly a result of the desire to use less expensive clocks as compared with the highly accurate and expensive satellite clocks. (The satellite clocks are still prone to the same types of errors but to less of an extent.) For this reason, the receiver clock errors are a much larger source of pseudo-range error than the satellite clock errors. Also, the GPS ground control station can monitor satellite clock errors and determine correction factors (which are uploaded to the satellites and relayed in the satellite message) to adjust the time reference. The precise time standard plays a very important role in use of GPS. However, a GPS receiver must keep track of its own clock errors. This seemingly undesirable feature is resolved because it is possible to estimate the clock errors accurately. With four satellites in view, it is possible to generate four equations in four unknowns; that is, three-dimensional position and receiver clock offset. By solving these equations

simultaneously, the unknowns are determined. (This is in itself another Kalman filtering problem but need not be considered when GPS is used as an aiding source.)

Thus, GPS by itself can be used to provide discrete position, velocity and time estimates. This research is only interested in using GPS as an aiding source to an INS. The joining together of the two systems brings together the best and suppresses the undesirable characteristics of both systems. The navigation solutions supplied by GPS are highly accurate but only become available as fast as the receiver computer can solve the problem. There also may be problems with poor satellite geometry which may lead to dilution of precision or even singular (unsolvable) situations in the navigation solution. Total dependence on satellite navigation may be risky in military situations in the presence of signal jamming. The main advantage of the INS is that it offers fairly accurate continuous navigation information. The drawback is that the accuracy will decrease with time because of gyro and accelerometer drifts which introduce random position and velocity errors into the system. By using GPS as an aiding source, the errors can be estimated and the INS can be reset often enough to keep the errors small. The resetting problem will not be considered in this research.

C. Problem Definition

The purpose of this research will be to compare the relative accuracy of a GPS aided INS using the two different measurement models

for processing the range rate observables. Typically, the "best" system would be the one where the mean square values (the variances for zero mean processes) of the INS errors are the smallest. The error covariance of the random process being estimated with the Kalman filter is updated at each point in time when a measurement is processed. The elements along the main diagonal of the error covariance matrix are the variances of each of the state variables. The updating of the error covariance does not depend on the actual measurements, so it is possible to calculate the error covariance over enough steps to determine the steady state standard deviation of the elements of the state vector.

The model which assumes the delta-range observable is a point measure of relative velocity will be referred to as the velocity model. The delayed state model will represent the model that equates the delta-range observable to the integral of relative velocity over the integration interval. The Kalman filter for the velocity model will yield overly optimistic error covariances because it is told that a valuable instantaneous velocity error is available. (This is the fault of the filter designer and not the Kalman filter.) For this reason, the "better" of the two models cannot be distinguished by finding the filter with the smallest standard deviation of the state variables as indicated by the calculated error covariance matrix. One could find the statistical properties of the state variables by using Monte Carlo type simulation methods, but this would be doing things the hard way. The method used in this research is suboptimal gain substitution (also known as suboptimal error analysis).

The Kalman gain is the residual weighting matrix which minimizes the elements along the main diagonal of the error covariance matrix. By definition, cycling any other gains through the Kalman filter equations will result in larger main diagonal elements, which in this case corresponds to a larger variance for the INS and GPS errors. The degree of suboptimallity of the velocity model can be found by using the Kalman gains from the velocity model as the gains in the delayed state model. The difference between the optimal and the suboptimal variances should increase as the delta-range integration interval is increased. However, as this time interval is decreased, the velocity model will become a better approximation of the delayed state model. This will be shown mathematically as well as experimentally.

In order to perform the model comparison and gain substitution, both the velocity model and the delayed state model must have the same process model. The statistics of the noise which drives the state equations in both models will be the same. Also, the measurement equations will be scaled so that they are in the same units which will make the gain substitution easier. The measurement noise statistics will also be the same in both models.

It should be noted that the RMS values of the system errors being estimated in this research do not represent the absolute accuracy of the "best" GPS aided INS. Instead, a simple model that is representative of a typical GPS aided INS will be used. Only the INS x,y,z position and velocity errors and the GPS receiver clock offset and fractional frequency errors will be modelled as state variables. This

is justified since these represent the dominant system errors. In the
Kalman filter, all process and measurement noises will be considered
to be Gaussian and white. For simulating the satellite coordinates,
a circular orbit will be assumed. By knowing the satellite spacing,
the inclination angles and the orbital period it is straightforward to
determine the satellites that are visible at a specified earth location.
These simplifications are justified because this research is directed
only toward the relative accuracy between the systems, with all condi-
tions equal except for the measurement equations.

II. KALMAN FILTER DESIGN

A. Linearized Measurement Equations

1. Aided inertial system block diagram

Figure 2 is the block diagram of the aided INS to be used for this study. The block labelled INS contains the gyros, accelerometers, and any other processors required to output the position and velocity of the vehicle in a given three-dimensional coordinate frame on a continuous basis. The aiding source block receives and decodes the GPS signals. It will be assumed that within a certain time interval, four pseudo-range and four delta-range measurements and the needed timing and satellite position information are available at the output of this block.

The difference operation shown is somewhat misleading in that this section of the system takes the difference between the measurement obtained with the aiding source (pseudo-range and delta-range) and the INS computed measurement, and not the actual position and velocity estimates as might be implied by the diagram. The computed pseudo-range is determined in this block using the current INS position, the satellite position, and the estimated clock offset. If the delayed state model is used, the computed delta-range is obtained here using the current and previous INS position estimates and the current and previous clock offset estimates. If the velocity model is used, the delta-range will be computed using the INS velocity and the estimated clock fractional frequency. The output of the block will be the eight-tuple which is the

difference of the INS computed and GPS measured quantities regardless of which measurement model is used. This will become the current input to the Kalman filter.

The Kalman filter observables will be noisy measurements related to the INS errors and the receiver clock errors. The job of the Kalman filter is to use this measurement to estimate the INS errors. The Kalman filter output will be subtracted from the total INS position and velocity output to yield the improved estimates. The receiver clock error estimates are used to update the receiver time reference (even though this operation is not implied from the block diagram). The measurement equation of the Kalman filter will now be derived.
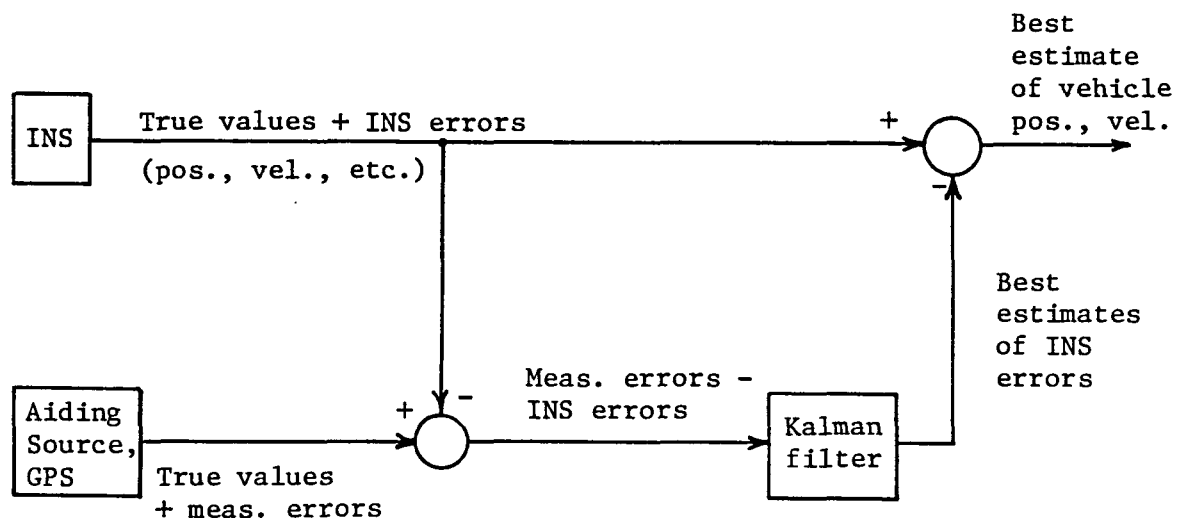

Figure 2. Aided INS block diagram

2. Baseline model

The baseline measurement equation accounts for the four pseudo-range measurements. The pseudo-range obtained from the code position

measurement is the true range plus the sum of the error due to the receiver clock offset and the measurement noise. The pseudo-range measurement at time t is:

$$z(t) = \rho_{true}(t) + cT(t) + v(t) \tag{1}$$

where

ρ_{true} : true distance from vehicle to the satellite

$$\rho_{true} = \sqrt{(x_s - x)^2 + (y_s - y)^2 + (z_s - z)^2}$$

x,y,z : true position

x_s, y_s, z_s : satellite coordinates

c : speed of light

T(t) : clock offset

v(t) : measurement noise

The range equation is nonlinear and needs to be linearized to fit the Kalman filter measurement equation format. A more general form for the measurement is:

$$z(t) = h(x,y,z,T,t) + v(t) \tag{2}$$

It is possible to linearize the equation about a nominal trajectory that does not depend on the actual measurement sequence. This produces a linearized Kalman filter [3]. The true position and clock offset variables can be written as:

$$x(t) = x^*(t) + \Delta x(t) \tag{3}$$
$$y(t) = y^*(t) + \Delta y(t) \tag{4a}$$

$$z(t) = z^*(t) + \Delta z(t) \tag{4b}$$

$$T(t) = T^*(t) + \Delta T(t) \tag{5}$$

The starred quantities are the approximate trajectories and the delta variables represent the errors between the true and the nominal trajectories. By using a Taylor series expansion about the nominal trajectory and retaining only first order terms, the linearized measurement equation has the following form:

$$z(t) - h(x^*,y^*,z^*,T^*,t) = \frac{\partial (h)}{\partial x}\bigg|_{x=x^*} \Delta x(t) + \frac{\partial (h)}{\partial y}\bigg|_{y=y^*} \Delta y(t) +$$

$$\frac{\partial (h)}{\partial z}\bigg|_{z=z^*} \Delta z(t) + \frac{\partial (h)}{\partial T}\bigg|_{T=T^*} \Delta T(t) + v(t) \tag{6}$$

$$z(t) - h(x^*,y^*,z^*,T^*,t) = (-1/\rho^*)(x_s - x)\Delta x(t) + (-1/\rho^*)(y_s - y)\Delta y(t)$$

$$+ (-1/\rho^*)(z_s - z)\Delta z(t) + c\Delta T(t) + v(t) \tag{7}$$

$$\rho^* = \sqrt{(x_s - x^*)^2 + (y_s - y^*)^2 + (z_s - z^*)^2} \tag{8}$$

The coefficients of the position errors in equation 7 are the cosines of the angles between the line-of-sight range vector and the x,y,z coordinate axes and are referred to as the direction cosines. The method for bringing the satellite and vehicle coordinates into the same coordinate frame and obtaining the direction cosines is given in Appendix B. Equation 7 can be rewritten as:

$$z(t) - h(x^*,y^*,z^*,T^*,t) = -\cos\theta_{x\rho}(t)\Delta x(t) - \cos\theta_{y\rho}(t)\Delta y(t)$$

$$- \cos\theta_{z\rho}(t)\Delta y(t) + c\Delta T(t) + v(t) \tag{9}$$

The measurement available to the Kalman filter is the difference of a measured quantity and a corresponding computed quantity. The linearized measurement model is the sum of a linear function of the error quantities and of the measurement noise. Equation 9 represents the baseline measurement model that the delta-range measurements will be appended onto.

3. Delayed state model

The Doppler shift of the GPS carrier is proportional to the relative velocity as shown in equation 10.

$$f_d = f_r - f_o = -(f_o/c)\dot{\rho} \qquad (10)$$

where

f_d : Doppler shift

f_o : transmitted carrier frequency

f_r : received carrier frequency

$\dot{\rho}$: time derivative of ρ

The GPS receiver measures the average of the Doppler shift by observing the phase change needed to keep the locally generated radio-frequency signal in phase with the received signal over a certain small time interval. The true Doppler count measurement is the integral of the Doppler shift as shown in equation 11 and has units of cycles.

$$N(t) = \int_{t_{n-1}}^{t_n} f_d \, dt = -f_o/c \int_{t_{n-1}}^{t_n} \dot{\rho} \, dt = -f_o/c [\rho(t_n) - \rho(t_{n-1})] \qquad (11)$$

Equation 11 is a nonlinear function with respect to the vehicle coordinates. The expression can be linearized about a nominal trajectory using the same method described above to linearize the pseudo-range measurement. The general form of the measurement is the same as equation 2. The corresponding h is:

$$h(x,y,z,T,t) = -f_o/c[\rho(t_n) - \rho(t_{n-1})] \tag{12}$$

where

$$\rho = \sqrt{(x_s - x)^2 + (y_s - y)^2 + (z_s - z)^2} + cT \tag{13}$$

Using equations 2-5, 12, and 13 and a Taylor series expansion of $h(x,y,z,T,t)$ about a nominal trajectory, the difference between the measured and the nominal Doppler count, to a first order approximation, is given as:

$$z - h(x^*,y^*,z^*,T^*,t) = -f_o/c[-\cos \theta_{x\rho}(t_n)\Delta x(t_n) - \cos \theta_{y\rho}(t_n)\Delta y(t)$$

$$- \cos \theta_{z\rho}(t_n)\Delta z(t) + c\Delta T(t_n) + \cos \theta_{x\rho}(t_{n-1})\Delta x(t_{n-1})$$

$$+ \cos \theta_{y\rho}(t_{n-1})\Delta y(t_{n-1}) + \cos \theta_{z\rho}(t_{n-1})\Delta z(t_{n-1})$$

$$- c\Delta T(t_{n-1})] + v(t) \tag{14}$$

Equation 14 is not in the usual form for the Kalman filter measurement equation. The reason is that the measurement is related to the past, as well as present error quantities. The usual Kalman filter equation only allows for connections of the current measurement to the current state. This is not an unsurmountable problem, though. The

delayed state Kalman filter has been developed to handle this type of measurement situation. It is a routine task to develop the corresponding delayed state Kalman filter recursive equations [3].

4. Velocity model

In the velocity model, the Doppler shift measurement is considered to be proportional to the instantaneous relative velocity between the vehicle and the satellite. Equation 10 gives the relationship between the true Doppler shift and the relative velocity.

Using the formula for the pseudo-range given in equation 1 (less the measurement noise), the time derivative of the pseudo-range is given as:

$$\dot{\rho} = -(1/\rho)(x_s - x)\dot{x} - (1/\rho)(y_s - y)\dot{y} - (1/\rho)(z_s - z)\dot{z} + c\dot{T} \qquad (15)$$

where

$\dot{x}, \dot{y}, \dot{z}$: vehicle velocity in the x,y,z directions

$\dot{T}$: receiver clock fractional frequency

The $\dot{\rho}$ equation is nonlinear in the vehicle coordinates. The equation may be put in the following general form:

$$z = h(x,y,z,\dot{x},\dot{y},\dot{z},\dot{T},t) + v(t) \qquad (16)$$

$$h = -f_o/c\dot{\rho} \qquad (17)$$

The velocity coordinates can be defined in terms of the nominal velocity trajectories and the velocity errors as:

$$\dot{x} = \dot{x}^* + \Delta\dot{x} \qquad (18)$$

$$\dot{y} = \dot{y}^* + \Delta\dot{y} \qquad (19)$$

$$\dot{z} = \dot{z}^* + \Delta\dot{z} \qquad (20)$$

Using a Taylor series expansion of h about the nominal trajectory and neglecting terms higher than first order, equation 16 can be rewritten as:

$$z - h(x^*,y^*,z^*,\dot{x}^*,\dot{y}^*,\dot{z}^*,\dot{T}^*,t) = \frac{\partial(h)}{\partial x}\bigg|_{x=x^*}\Delta x + \frac{\partial(h)}{\partial y}\bigg|_{y=y^*}\Delta y$$

$$+ \frac{\partial(h)}{\partial z}\bigg|_{z=z^*}\Delta z + \frac{\partial(h)}{\partial \dot{x}}\bigg|_{\dot{x}=\dot{x}^*}\Delta\dot{x} + \frac{\partial(h)}{\partial \dot{y}}\bigg|_{\dot{y}=\dot{y}^*}\Delta\dot{y} + \frac{\partial(h)}{\partial \dot{z}}\bigg|_{\dot{z}=\dot{z}^*}\Delta\dot{z}$$

$$+ \frac{\partial(h)}{\partial \dot{T}}\bigg|_{\dot{T}=\dot{T}^*}\Delta\dot{T} + v(t) \qquad (21)$$

The first three terms on the right hand side of equation 21 can be neglected because these terms turn out to be many orders of magnitude less than the other terms in this expression. This result may not be true in general but in this case the assumption is valid because of the large GPS orbital radius. If the required partial derivatives are performed and the terms proportional to the position errors are neglected, equation 21 becomes:

$$z(t) - h(x^*,y^*,z^*,\dot{x}^*,\dot{y}^*,\dot{z}^*,\dot{T}^*,t) = -f_o/c[-\cos\theta_{x\rho}(t_n)\Delta\dot{x}(t)$$

$$- \cos\theta_{y\rho}(t)\Delta\dot{y}(t) - \cos\theta_{z\rho}(t)\Delta\dot{z}(t) + c\Delta\dot{T}(t)] + v(t) \qquad (22)$$

The linearized measurement model is the difference of the receiver

Doppler shift measurement and the predicted Doppler shift computed along the nominal trajectory. The model was derived on the assumption that the receiver can make an instantaneous relative velocity measurement, which is physically impossible. Therefore, this is a fictitious model. However, in the limit as the delta-range integration interval goes to zero, the form of the delayed state model (which is the legitimate model) approaches the form of the velocity model. This is shown in Appendix A.

B. Kalman Filter Modelling

1. State equation

It is clear that the vehicle position and velocity errors and the GPS receiver clock offset and fractional frequency errors are the random variables that need to be estimated from the linearized measurements discussed above. These eight random variables will be the state variables in the Kalman filter. The job of the Kalman filter is to accept the linearized measurements and provide the best estimate of the state variables based on the known statistical properties of the measurement noise and the noise that drives the random process. The process equation of the Kalman filter defines the dynamic properties of the state variables when they are driven by Gaussian white noise. Once the process and measurement equations and the corresponding noise statistics are defined, the modelling is complete and the required Kalman filter parameters may be found. The process equation will be considered next.

Typically, position and velocity in a single direction are obtained by integrating the output of an accelerometer as shown in figure 3. The

output of the accelerometer will be the true acceleration plus additive noise. The output of the first integrator will be the true velocity plus the velocity error due to the random accelerometer error. The output of the second integrator is the sum of the true position plus a position error which is the result of the propagation of the accelerometer noise through the system. The model used for the error propagation will be the double integrator plant shown in Figure 4. The input will be assumed to be Gaussian white noise. The same model will be used to define the error propagation in the x, y, and z directions. The state variable assignments are as follows:

$$x_1 = \Delta x \; : \; \text{x position error}$$

$$x_2 = \Delta \dot{x} \; : \; \text{x velocity error}$$

$$x_3 = \Delta y \; : \; \text{y position error}$$

$$x_4 = \Delta \dot{y} \; : \; \text{y velocity error} \tag{23}$$

$$x_5 = \Delta z \; : \; \text{z position error}$$

$$x_6 = \Delta \dot{z} \; : \; \text{z velocity error}$$

The plant equations for the given state variable assignments are:

$$\dot{x}_1 = x_2 \; , \quad \dot{x}_2 = f_1(t)$$

$$\dot{x}_3 = x_4 \; , \quad \dot{x}_4 = f_2(t) \tag{24}$$

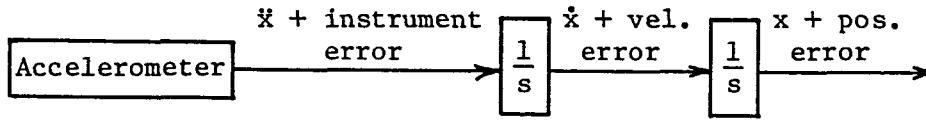$$\dot{x}_5 = x_6 \; , \quad \dot{x}_6 = f_3(t)$$

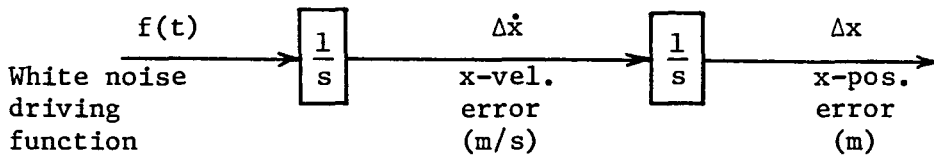Figure 3. Instrumentation error propagation

Figure 4. State variable dynamics in the x-direction

The position errors have units of meters and the velocity errors have units of meters per second. The velocity errors are modelled as a Wiener process (integrated Gaussian white noise). This allows for random walk of the velocity errors. The velocity and position errors will be Gaussian, zero mean, nonstationary, random processes.

The accuracy of GPS is highly dependent on a precise time reference for such things as time tagging the satellite transmissions and measuring pseudo-range. For economic reasons, commercial receivers cannot rely on highly stable clocks as the satellites do. Instead, the receiver keeps track of the offset and fractional frequency of its own clock so that the receiver can compensate for the mild instability. For example, the computed pseudo-range uses the best available measurement of the clock offset to compare with the measured pseudo-range which is affected by the true clock offset. Suppose that the current

position was known perfectly, then the linearized pseudo-range would only be the sum of the range errors due to clock offset error and the measurement noise. The clock error could be estimated and used to correct the current estimate of the clock offset. This is analogous to keeping track of time with a watch that runs fast by keeping track of the offset. If an accurate reference is available, the offset estimate may be improved and the correct time is found by subtracting out the best estimate of the offset.

There has been a considerable amount of research done on the modelling of clock noise and its statistical properties (the so-called Allan variances) [10]. The single-sided power spectral density function of fractional frequency fluctuations is modelled empirically with a polynomial that contains powers of the independent variable (frequency) as shown in equation 25.

$$S(f) = h_{-2}f^{-2} + h_{-1}f^{-1} + h_0f^0 + h_1f^1 + h_2f^2 \tag{25}$$

where

h_{-2} = random walk frequency noise

h_{-1} = flicker frequency noise

h_0 = white frequency noise

h_1 = flicker phase noise

h_2 = white phase noise

Each of the coefficients represents a different type of clock error. For high precision systems, effects of flicker noise must be modelled. However, this leads to a spectral density function with

terms that are not a function of frequency squared. If spectral

factorization is performed, the resulting functions cannot be put in

state space form in an exact manner (that is without adding extra

state variables to approximate the true function). There has been an

expressed desire to use only a second order model for the clock error.

Since the other more advanced models are approximations, it is justified

to use the second order model approximation which does account for the

clock offset error and the clock fractional frequency error which are

much more crucial than the flicker noise error. Thus, only the h_0 and

h_{-2} terms will be included. A covariance model which includes the h_{-2},

h_{-1}, and h_0 parameters has been derived [10]. The model used in this

research will take advantage of this model except that the effects of

the flicker noise will be neglected. The model used is the double

integrator plant where there are white noise inputs into both

integrators and will lead to the desired covariance model when the

flicker noise is not included. (There are many subtleties involved in

the covariance expression derivation, but they need not be dealt with

here.) The clock offset error is random walk plus integrated random

walk and the clock fractional frequency error is also random walk as

shown in Figure 5. Once again, the output of the integrators are the

state variables and are defined below.

$$x_7 = \Delta T : \text{clock offset error}$$

$$x_8 = \Delta\dot{T} : \text{clock frequency fluctuation error}$$

(26)

where

x_7 : has units of seconds

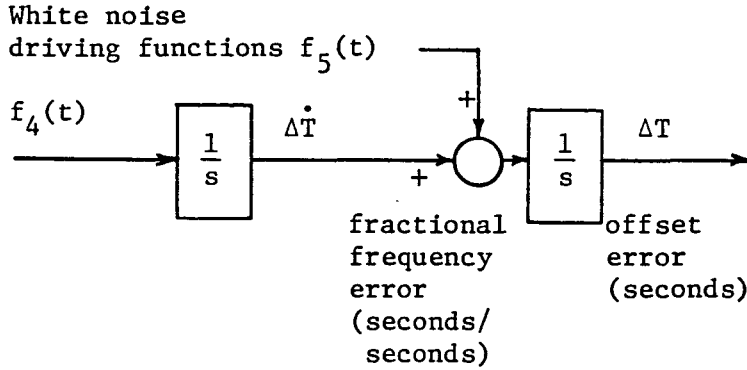x_8 : has units of seconds/seconds or fractional frequency

Figure 5. Clock error propagation model

The following equations describe the plant for the state variable assignments of equation 26.

$$\dot{x}_7 = x_8 + f_5(t), \quad \dot{x}_8 = f_4(t) \tag{27}$$

Since this research is concerned with relative accuracy between measurement models, this model is adequate because it contains the clock error state required in both models and the relationship between the two clock error state variables.

The continuous state equation for the state variable assignments given in equations 24 and 27 has the following form:

$$\dot{x}(t) = F(t)x(t) + G(t)w(t) \tag{28}$$

where $x(t)$: (nx1) process state vector

F(t) : (nxn) matrix

G(t) : (nxp) input distribution matrix

w(t) : (pxl) white noise input vector

$$
F(t) = \begin{bmatrix} 0 & 1 & 0 & 0 & 0 & 0 & 0 & 0 \\ 0 & 0 & 0 & 0 & 0 & 0 & 0 & 0 \\ 0 & 0 & 0 & 1 & 0 & 0 & 0 & 0 \\ 0 & 0 & 0 & 0 & 0 & 0 & 0 & 0 \\ 0 & 0 & 0 & 0 & 0 & 1 & 0 & 0 \\ 0 & 0 & 0 & 0 & 0 & 0 & 0 & 0 \\ 0 & 0 & 0 & 0 & 0 & 0 & 0 & 1 \\ 0 & 0 & 0 & 0 & 0 & 0 & 0 & 0 \end{bmatrix}, \; G(t) = \begin{bmatrix} 0 & 0 & 0 & 0 & 0 \\ 1 & 0 & 0 & 0 & 0 \\ 0 & 0 & 0 & 0 & 0 \\ 0 & 1 & 0 & 0 & 0 \\ 0 & 0 & 0 & 0 & 0 \\ 0 & 0 & 1 & 0 & 0 \\ 0 & 0 & 0 & 0 & 1 \\ 0 & 0 & 0 & 1 & 0 \end{bmatrix}, \; w(t) = \begin{bmatrix} f_1(t) \\ f_2(t) \\ f_3(t) \\ f_4(t) \\ f_5(t) \end{bmatrix} \quad (29)
$$

Since the aiding source measurements are available only in discrete time, the corresponding discrete-time process equation of equation 28 must be formulated as follows [3]:

$$
x(k+1) = \Phi(k)x(k) + w(k) \quad (30)
$$

where $x(k)$: (nxl) process state vector

$\Phi(k)$: (nxn) state transition matrix which describes the homogeneous trajectory of $x(k)$ from k to k+1

$w(k)$: (nxl) Gaussian white noise sequence vector; the driven response at k+1 due to presence of white noise over the interval from k to k+1

The x,y,z and clock errors are uncorrelated and have the same transition matrix for the double integrator plant for a step-size Δt

$$
\Phi(k) = \begin{bmatrix} 1 & \Delta t \\ 0 & 1 \end{bmatrix} \quad (31)
$$

The total transition matrix will be block-diagonal in form and will be the null matrix except along the main diagonal which will consist of four 2x2 matrices in the form of equation 31.

Another parameter needed in the formulation of the random process being modelled is the Q matrix [3]. This quantity describes the covariance structure of the white sequence vector $w(k)$. The definition of the $Q(k)$ matrix is given as:

$$E[w(k)w^T(i)] = \begin{cases} Q(k) & \text{for } k=i \\ 0 & \text{for } k \neq i \end{cases} \tag{32}$$

where $E[\ \ ]$: is the expected value operator.

Because the x,y,z and clock errors are uncorrelated, the total $Q(k)$ matrix has the following block diagonal form (same as the transition matrix):

$$Q(k) = \begin{bmatrix} Q_1 & 0 & 0 & 0 \\ 0 & Q_2 & 0 & 0 \\ 0 & 0 & Q_3 & 0 \\ 0 & 0 & 0 & Q_4 \end{bmatrix} \tag{33}$$

$$Q_i(k) = \begin{bmatrix} A_i \dfrac{(\Delta t)^3}{3} & A_i \dfrac{(\Delta t)^2}{2} \\ A_i \dfrac{(\Delta t)^2}{2} & A_i \Delta t \end{bmatrix} \qquad i = 1,2,3$$

and

$$Q_4(k) = \begin{bmatrix} A_4\dfrac{(\Delta t)^3}{3} + A_5\Delta t & A_4\dfrac{(\Delta t)^2}{2} \\ \\ A_4\dfrac{(\Delta t)^2}{2} & A_4\Delta t \end{bmatrix}$$

The constants A_1 – A_5 represent the power spectral density ampli-
tudes of the driving terms $f_1(t)$ – $f_5(t)$. The process is completely
defined (as far as the Kalman filter is concerned) with the parameters
$\Phi(k)$ and $Q(k)$. Now that the state is defined, the discrete Kalman
filter measurement equation may be developed.

2. <u>Measurement equation</u>

Two different measurement formats are needed. The first is the
usual Kalman filter measurement equation. The other is for the delayed
state Kalman filter. The baseline measurements (four pseudo-ranges)
and the velocity (Doppler) measurements can be made to fit the form of
the usual measurement equation. The Doppler measurements which are
treated correctly as the integral of Doppler shift will use the delayed
state measurement form.

The usual Kalman filter measurement equation has the following
form [3]:

$$z(k) = H(k)x(k) + v(k) \tag{34}$$

where $z(k)$ = (mx1) measurement vector

$\mathbf{H}(k)$ = (mxn) matrix which gives the ideal connection between the current measurement and the current state

$\mathbf{v}(k)$ = (mxl) white measurement noise sequence assumed to be uncorrelated with $\mathbf{w}(k)$, that is $E[\mathbf{w}(k)\mathbf{v}^T(1)] = 0$ for all k and l

The covariance structure of $\mathbf{v}(k)$ is defined as:

$$E[\mathbf{v}(k)\mathbf{v}^T(i)] = \begin{cases} R(k) & k=i \\ 0 & k \neq i \end{cases} \tag{35}$$

The baseline measurements $\mathbf{z}(k)$ are the pseudo-range measurements. The first four rows of the connection matrix $\mathbf{H}(k)$ will have the following form:

$$\mathbf{H}_i(k) = [-\cos\theta_{x\rho}(k)_i \quad 0 \quad -\cos\theta_{y\rho}(k)_i \quad 0 \quad -\cos\theta_{z\rho}(k)_i \quad 0 \quad c \quad 0] \tag{36}$$

where $i=1,2,3,4$: direction cosines for each satellite

The velocity model is obtained by augmenting the baseline measurement model with the four linearized Doppler measurements. If the linearized velocity model given in equation 22 is multiplied by the delta-range integration interval (in seconds), the units of the resulting equation will be cycles. The velocity measurement model will then have the same units as the delayed state model. Since the origin of the Doppler measurement is the difference of the phase required to track the received carrier over a small time interval, the units of the measurement should be cycles regardless of the measurement model that is used. The fifth through the eighth rows of the connection

matrix for the ith satellite are:

$$H_i(k) = [0 \quad -(\Delta t/\lambda_0)\cos\theta_{x\rho}(k)_i \quad 0 \quad -(\Delta t/\lambda_0)\cos\theta_{y\rho}(k)_i$$

$$0 \quad -(\Delta t/\lambda_0)\cos\theta_{z\rho}(k)_i \quad 0 \quad f_0\Delta t] \tag{37}$$

where $i : 1,2,3,4$

   λ_0 : wavelength of carrier

The form of the delayed state Kalman filter measurement equation is given as [3]:

$$z(k) = H(k)x(k) + J(k)x(k-1) + v(k) \tag{38}$$

where $J(k)$ = (mxn) matrix which gives the connection between the current measurement and the previous state vector

(The other variables in equation 38 are defined above.)

The connection matrices for the delayed state model will now be defined. (The development of these matrices is discussed further in Appendix A.) The first four measurements are the linearized pseudo-ranges so that the first four rows of $H(k)$ are the same as those defined in equation 36. The first four rows of $J(k)$ will be zero. The last four rows of $H(k)$ and $J(k)$ are obtained from equation 14. The fifth through the eighth rows of $H(k)$ and $J(k)$ for the ith satellite are given by:

$$H_i(k) = [-(1/\lambda_0)\cos\theta_{x\rho}(k)_i \quad 0 \quad -(1/\lambda_0)\cos\theta_{y\rho}(k)_i$$

$$0 \quad -(1/\lambda_0)\cos\theta_{z\rho}(k)_i \quad 0 \quad f_0 \quad 0] \tag{39}$$

$$J_i(k) = [-(1/\lambda_0)\cos\theta_{x\rho}(k-1)_i \quad 0 \quad -(1/\lambda_0)\cos\theta_{y\rho}(k-1)_i$$

$$0 \quad -(1/\lambda_0)\cos\theta_{z\rho}(k-1)_i \quad 0 \quad f_0 \quad 0] \tag{40}$$

where $\qquad$ i = 1,2,3,4

The required Kalman filter modelling is complete when the parameters $\Phi(k)$, $Q(k)$, $H(k)$, $J(k)$, and $R(k)$ are defined. The power spectral density of the noise that drives the process equation and the covariance of the measurement noise are considered as given by the filter designer. These parameters must be chosen with care to fit the situation at hand. With these parameters, the designer can affect the resulting error covariance to achieve almost any range of accuracy during error covariance analysis. Whether this corresponds to the real life situation is the important consideration. If empirical data from the actual system are not available, the designer must rely on intuition to determine reasonable parameters.

C. Kalman Filter Recursive Equations

At this point, it is appropriate to describe the recursive Kalman estimator. The update equation is used to calculate the best estimate of the current state by adding to the a priori estimate a weighted sum of the current measurement residuals. The update equation for the delayed state filter is given in equation 41.

$$\hat{x}(k) = \hat{x}^-(k) + K(k)[z(k) - H(k)\hat{x}^-(k) - J(k)\hat{x}(k-1)] \tag{41}$$

where $\qquad \hat{x}(k)$: best estimate at t=k of $x(k)$; the hat notation

denotes an estimated quantity, also known as the

a posteriori estimate at t=k

$\hat{\bar{x}}(k)$: best estimate of $x(k)$ computed at previous step

$K(k)$: weighting matrix, also known as the gain

The expression inside the brackets is the measurement residual. The

vector $z(k)$ is the input to the filter and the terms following it are

the best estimate of what the measurement should be as determined by

the measurement equation. The noise term is left out here since it is

assumed to have a zero mean.

The Kalman gain is the weighting matrix that minimizes the mean

square estimation error. The estimation error is defined as the differ-

ence of the true state and the best a posteriori estimate of the state

as shown in equation 42 below.

$$e(k) = x(k) - \hat{x}(k) \qquad (42)$$

The error covariance matrix $P(k)$ is defined as:

$$P(k) = E[e(k)e^T(k)] \qquad (43)$$

With modest effort, $P(k)$ may be expanded (with appropriate substitutions)

to yield the general error covariance expression for the delayed state

Kalman filter which is given as [3]:

$$P(k) = P^-(k) - K(k)[H(k)P^-(k) + J(k)P(k-1)\Phi^T(k-1)]$$

$$-[P^-(k)H^T(k) + \Phi(k-1)P(k-1)J^T(k)]K^T(k) + K(k)L(k)K^T(k) \qquad (44)$$

where

$$L(k) = H(k)P^-(k)H^T(k) + R(k) + J(k)P(k-1)J^T(k) +$$

$$H(k)\Phi(k-1)P(k-1)J^T(k) + J(k)P(k-1)\Phi^T(k-1)H^T(k) \qquad (45)$$

The Kalman gains are found by taking the matrix derivative of equation 44, setting it equal to the null matrix, and solving for the gain matrix which minimizes the elements along the major diagonal of $P(k)$. The result is:

$$K(k) = [P^-(k)H^T(k) + \Phi(k-1)P(k-1)J^T(k)]L(k)^{-1} \qquad (46)$$

If the Kalman gain is substituted back into equation 44, the error covariance (only in the case where the optimal gains are used) simplifies to:

$$P(k) = P^-(k) - K(k)L(k)K^T(k) \qquad (47)$$

To assimilate the current measurement with the update equation, the optimal gain and the a priori state estimate must be available. The Kalman gain depends on the a priori error covariance. The error co-variance projection equation provides the a priori error covariance matrix to be used in the gain equation on the next step. The state projection equation uses the process equation without the noise term to estimate the state at the next step. The projection equations are:

$$P^-(k+1) = \Phi(k)P(k)\Phi^T(k) + Q(k) \qquad (48)$$

$$\hat{x}^-(k+1) = \Phi(k)\hat{x}(k) \qquad (49)$$

Equations 41 and 46-49 are the recursive equations that comprise the delayed state Kalman filter. Figure 6 shows the recursive nature of the filter. The input is the measurement stream z(k) and the initial conditions. The Kalman gain is computed using the a priori and previous error covariances. After the gains are found, the state and the error covariance are updated. These quantities are then projected ahead to be used in the next step. The output is the updated state estimate $\hat{x}$(k) and the associated error covariance P(k). The filter is recursive in that it is not required to save the measurements, all the previous states, or any other intermediate calculations. This information is transferred through the a priori state estimate and error covariance matrices. The delayed state Kalman filter does require the updated error covariance and state estimate to be saved to become P(k-1) on the next step. This is not required in the usual Kalman filter. The usual Kalman filter equations may be obtained by letting J(k) equal the null matrix in the delayed state filter equations. The resulting recursive equations are given in Figure 7 [3].

D. Kalman Filter Error Analysis

Notice that the measurement data have no effect on the determination of the error covariance. The Kalman filter loop may be executed without assimilating measurements if only the error covariance trajectory is desired. This provides the filter designer with an easy method to assess system accuracy as it is modelled. The recursive structure for calculating a sequence of error covariances is the same as the usual
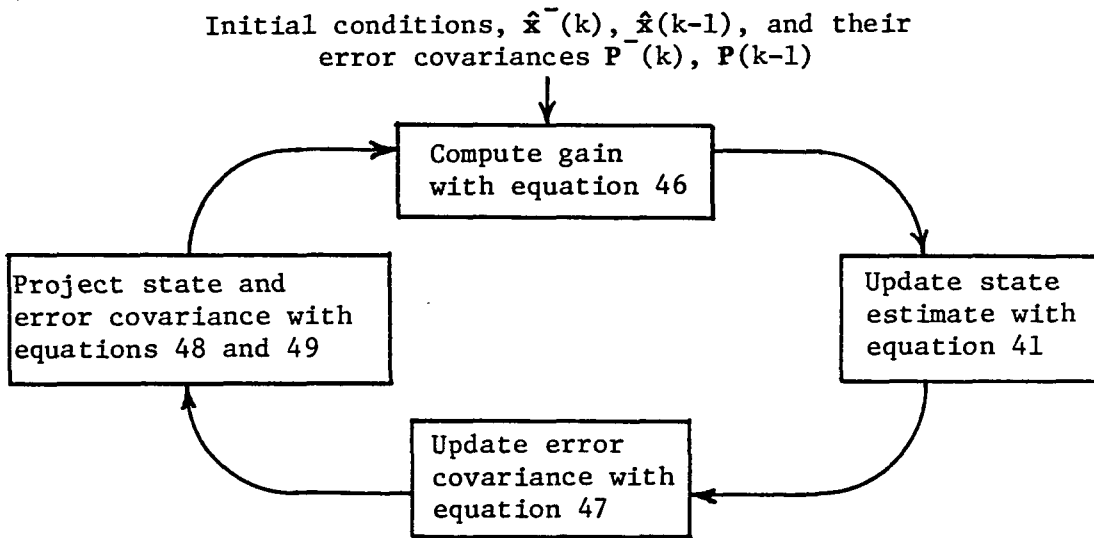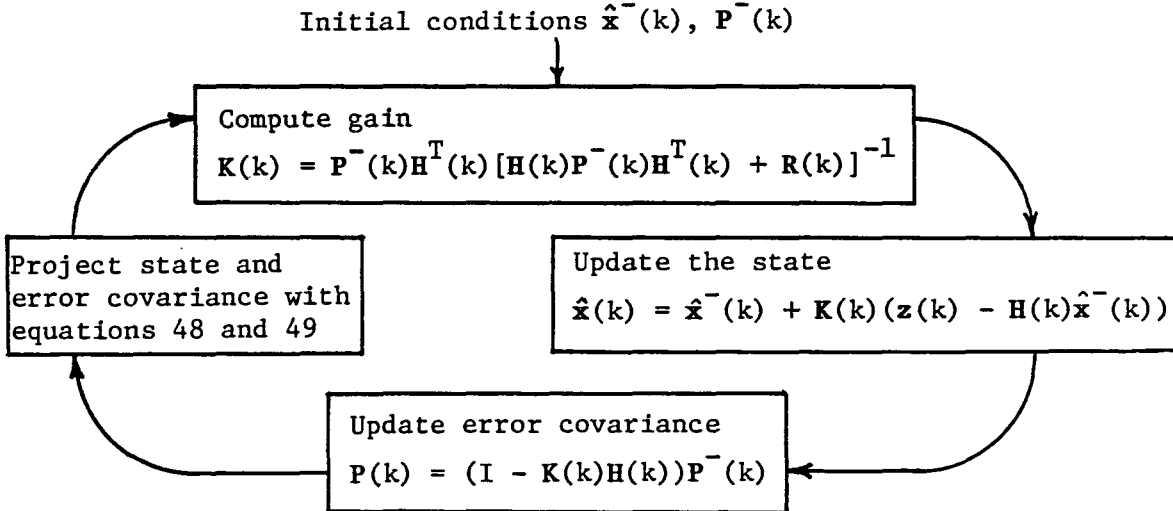
Initial conditions, $\hat{\mathbf{x}}^{-}(k)$, $\hat{\mathbf{x}}(k-1)$, and their
error covariances $\mathbf{P}^{-}(k)$, $\mathbf{P}(k-1)$

```
                    ┌──────────────────┐
         ┌─────────→│ Compute gain     │──────────┐
         │          │ with equation 46 │          │
         │          └──────────────────┘          ↓
┌──────────────────┐                      ┌──────────────────┐
│ Project state and│                      │ Update state     │
│ error covariance │                      │ estimate with    │
│ with             │                      │ equation 41      │
│ equations 48 and 49                     └──────────────────┘
└──────────────────┘                              │
         ↑          ┌──────────────────┐          ↓
         └──────────│ Update error     │←─────────┘
                    │ covariance with  │
                    │ equation 47      │
                    └──────────────────┘
```

Figure 6.   Delayed state Kalman filter loop

Initial conditions $\hat{\mathbf{x}}^{-}(k)$, $\mathbf{P}^{-}(k)$

```
      ┌────────────────────────────────────────────────────────────────┐
 ┌───→│ Compute gain                                                   │───┐
 │    │ K(k) = P⁻(k)Hᵀ(k)[H(k)P⁻(k)Hᵀ(k) + R(k)]⁻¹                      │   │
 │    └────────────────────────────────────────────────────────────────┘   ↓
┌──────────────────┐                          ┌────────────────────────────────────┐
│ Project state and│                          │ Update the state                   │
│ error covariance │                          │ x̂(k) = x̂⁻(k) + K(k)(z(k) − H(k)x̂⁻(k))│
│ with             │                          └────────────────────────────────────┘
│ equations 48 and 49                                        │
└──────────────────┘                                         ↓
 ↑    ┌────────────────────────────────────────┐            │
 └────│ Update error covariance                │←───────────┘
      │ P(k) = (I − K(k)H(k))P⁻(k)              │
      └────────────────────────────────────────┘
```

Compute gain

$$K(k) = P^{-}(k)H^{T}(k)[H(k)P^{-}(k)H^{T}(k) + R(k)]^{-1}$$

Update the state

$$\hat{\mathbf{x}}(k) = \hat{\mathbf{x}}^{-}(k) + K(k)(z(k) - H(k)\hat{\mathbf{x}}^{-}(k))$$

Update error covariance

$$P(k) = (I - K(k)H(k))P^{-}(k)$$

Figure 7.   Usual Kalman filter loop

Kalman filter loop (as in Figures 6 and 7) except that the state update
calculation may be bypassed since this step has no effect on the error
covariance calculation.

In this research, there is a need to compare the relative accuracy between the delayed state and the velocity measurement models. Since the velocity model is considered to be a fictitious model, the determination of the better of the models may be inconclusive if the comparison is made on the basis of which has the smallest state variable mean square error. The method of comparison to be used in this research is suboptimal gain substitution. This method allows the filter designer to assess the relative degradation in system accuracy when an approximate measurement model is used instead of the true measurement model. The Kalman gains determined with the approximation model are used as the gains in what the designer believes to be the truth model. The general error covariance update expression must be used since the substituted gains will not be the Kalman gains for the truth model. The degree of suboptimallity of the approximate model may be found by noting the increase in the elements along the main diagonal of the error covariance matrix. The process required to perform the suboptimal error analysis is shown in Figure 8. Both filters are run in parallel except the gains for the truth model are obtained from the approximate model.
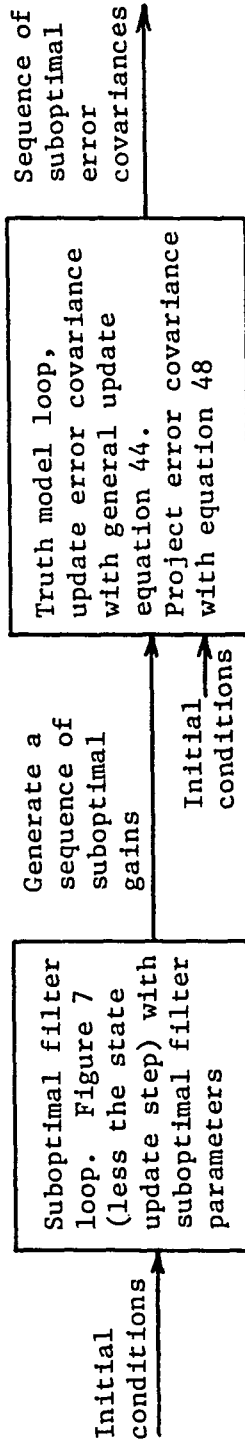
Figure 8. Suboptimal error analysis structure

III.   RESULTS

A.   Specification of Filter Parameters

In order to implement the Kalman filter equations, the GPS satellite and receiver positions must be simulated so that the time varying measurement connection matrices may be found at each time step. A typical GPS satellite constellation was chosen using the orbital information shown in Figure 1 [9]. If the vehicle starting position is chosen in the southwest United States near California (250 degrees east longitude, 30 degrees north latitude) at a certain time, satellites 5, 7, 10, and 15 should remain visible in this area enough time for the Kalman filter error covariance to reach a steady state condition if the initial error covariance is started out as the zero matrix (implies a perfect initial estimate of the state vector). Since the satellite positions are always assumed as given during normal tracking of the satellites, there is no loss in generality in assuming a circular one-half day orbit at the given angle of inclination and position in orbit. Table 1 gives the necessary angles to specify the initial satellite positions. (See Appendix B for further explanation.) The satellite and vehicle coordinates can be transferred into an earth centered, earth fixed frame of reference (ECEF). To put some dynamics into the problem, the vehicle is considered to be moving in an eastward direction at constant velocity and constant altitude and latitude. The velocity was chosen to be approximately 1700 miles per hour. This corresponds to an angular velocity which is half as fast as the

satellite angular velocity. (This speed was chosen somewhat arbitrarily but was made large enough to allow for a fair amount of change in the direction cosines over a time span of a few minutes.) For each satellite, it is a routine matter to generate the direction cosines for a given time. These terms will be used to load the measurement connection matrices.

Table 1. Satellite position angles (degrees)

Satellite	α	β	γ
5	60	55	160
7	120	55	80
10	180	55	120
15	240	55	40

The parameters $\Phi(k)$ and $Q(k)$ have been developed for the given state model in terms of the measurement interval (Δt) and the process noise power spectral densities. Different values for Δt will be used to compare the two measurement models. The smaller the time interval becomes, the better the velocity model should approximate the delayed state model. The comparison will be made for time intervals of one second and one-tenth of a second. The power spectral densities are chosen so that the amount of noise that enters the system (over the sampling interval) causes a reasonable amount of uncertainty in the state variables. For the x, y, and z errors, the power spectral

densities were chosen to be one hundred with units of meters squared per seconds cubed. After one second, this amount of noise leads to a RMS velocity error of ten meters per second and a RMS position error of approximately six meters. The power spectral densities for the clock model are chosen to correspond to a "poor" clock [10]. The units of h_0 are in seconds and the units of h_{-2} are in Hertz. This means that results obtained will not be dependent on a highly stable local clock. The power spectral densities for the five white noise inputs are given below:

$$A_1 = A_2 = A_3 = 100 \ (m^2/s^3) \ .$$

$$A_4 = h_0/2 \quad \text{where } h_0 = 9.43 \times 10^{-20} \ s$$

$$A_5 = 2(\pi)^2 h_{-2} \quad \text{where } h_{-2} = 3.80 \times 10^{-21} \ Hz$$

The R matrix elements correspond to the measurement noise covariances. It is assumed that the measurement noise associated with each of the four pseudo-range measurements is the same and has a RMS value of fifty meters. Measurement uncertainties due to satellite clock errors, ionospheric refraction delays, Costas loop errors and other unmodelled errors are all lumped into this quantity. It is common for phase lock loops to stay locked onto a received signal to within much less than a cycle. If a one cycle RMS measurement error was assumed, it would be possible to keep the velocity errors on the order of two-tenths of a meter per second (corresponds to one light wavelength over a one second interval). This type of accuracy seems a bit unreasonable,

though. A more realistic measurement error would include the effects of the unmodelled errors mentioned above. If the measurement error for the Doppler count measurement is taken as ten cycles, this will correspond to an RMS velocity error of about two meters per second. The measurement error variance used for the Doppler shift of each satellite signal is one hundred cycles squared for a sampling interval of one second. The R matrix for the one second measurement interval is given as:

$$
R(k) = \begin{bmatrix}
2500 & 0 & 0 & 0 & 0 & 0 & 0 & 0 \\
0 & 2500 & 0 & 0 & 0 & 0 & 0 & 0 \\
0 & 0 & 2500 & 0 & 0 & 0 & 0 & 0 \\
0 & 0 & 0 & 2500 & 0 & 0 & 0 & 0 \\
0 & 0 & 0 & 0 & 100 & 0 & 0 & 0 \\
0 & 0 & 0 & 0 & 0 & 100 & 0 & 0 \\
0 & 0 & 0 & 0 & 0 & 0 & 100 & 0 \\
0 & 0 & 0 & 0 & 0 & 0 & 0 & 100
\end{bmatrix} \tag{50}
$$

When the sampling interval is changed to one-tenth of a second, the measurement noise variance for the Doppler measurements is changed to 10000 and the pseudo-range measurement noise variance is left unchanged. All the Kalman filter parameters (H, J, Φ, Q, R) are now defined.

B. Program Results

Computer programs were developed to determine the steady state
error covariance for the baseline, delayed state and velocity models.
The baseline program uses only the pseudo-range measurements and is
called ERRAN1 (error analysis one). The delayed state and velocity
model programs are called ERRAN2 and ERRAN3, respectively. The program
which performs the gain substitution from the velocity model to the
delayed state model is called ERRAN4. Each of the programs contains
the same procedures for generating direction cosines. Matrix operations
are all performed with the same matrix multiply, transpose and inverse
procedures and were checked extensively with a test program before
being inserted into each of the four programs. As a check on the
delayed state and velocity model programs, the measurement noise vari-
ance associated with the Doppler measurements was made large to make
sure that the resulting error covariance "falls back" to the profile
determined with the baseline model. This tells the Kalman filter to
give little weight to the Doppler measurements. These tests were
successful.

The square roots of the elements along the main diagonal of the
error covariance matrix are the standard deviations of the state vari-
ables which represent the system errors. The standard deviations
of the position and clock offset errors (states 1, 3, 5, and 7) for
the baseline model and a one second measurement interval are given in
Figure 9. The velocity errors and fractional frequency error profiles
(states 2, 4, 6 and 8) are given in Figure 10. The standard deviations
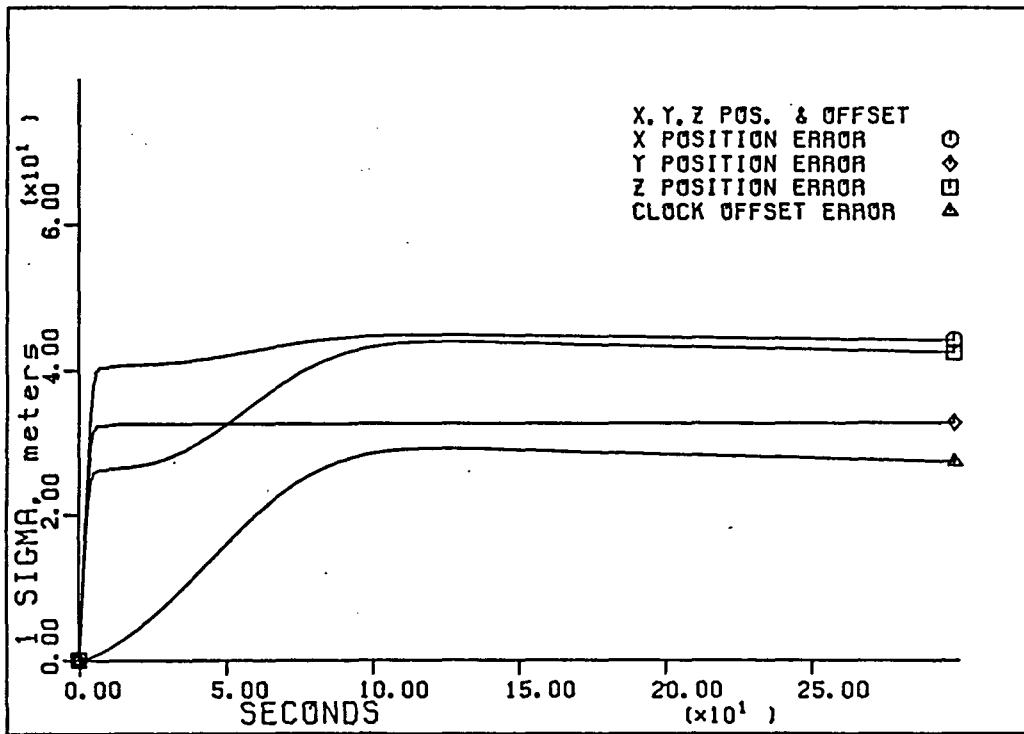
Figure 9.   x,y,z position and offset error profiles for $\Delta t = 1s$
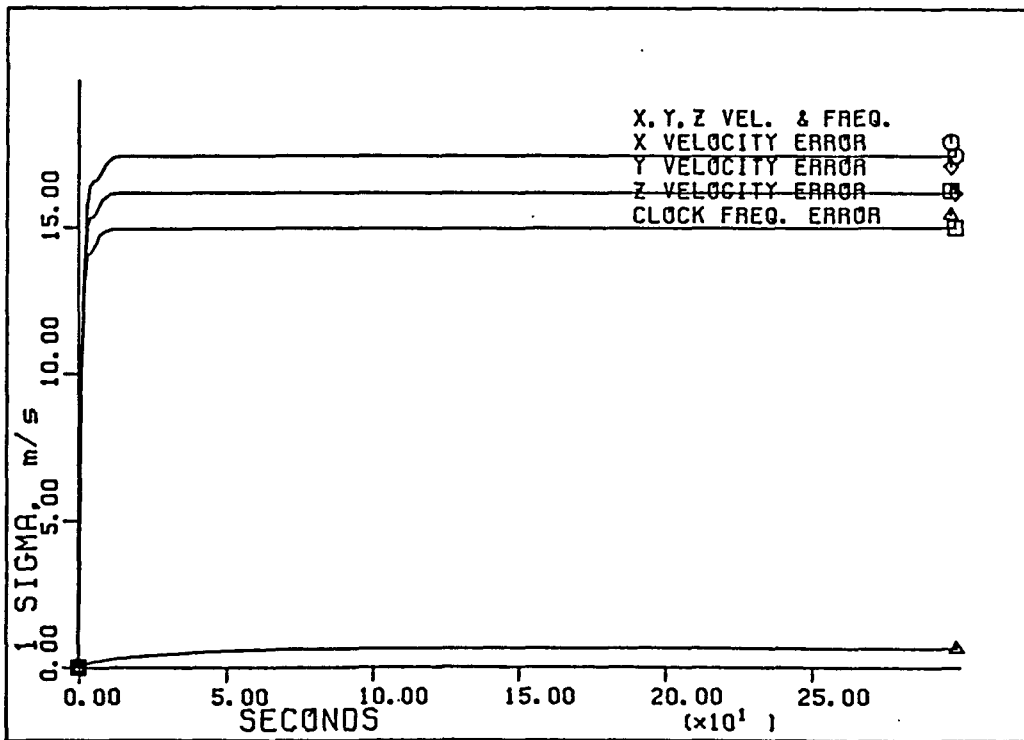
Figure 10.   x,y,z velocity and fractional frequency error profiles
for $\Delta t = 1s$

of the clock offset and fractional frequency errors are multiplied by
the speed of light to obtain the corresponding errors in position and
velocity units, respectively. The initial error covariance was the
null matrix. The resulting state standard deviation profiles start out
at the origin, go through a transient period, and then settle to "near"
steady state values.

The Kalman filters for the delayed state model, the velocity model
and the delayed state model with the gains from the velocity model were
each executed under the same initial conditions and the same noise
statistics. The profiles of the standard deviation of a particular
state variable from each of the three models are plotted together in
Figures 11-20. The sampling interval for these plots is one second.
For the position error states, the delayed state model had the smallest
standard deviation, followed by the velocity model. The delayed state
model with the suboptimal gains has the largest standard deviation.
Notice that this ordering is maintained throughout the complete
trajectory. For the velocity error states, the velocity model pre-
dicted the smallest standard deviation followed by the delayed state
model. The delayed state model with the suboptimal gains estimated the
largest standard deviation of the velocity error states.

The difference in the profiles for the clock offset and fractional
frequency errors determined from the three programs was too close to
be observed in Figures 17 and 19. Thus, the difference between the two
suboptimal trajectories and the optimal trajectory was plotted and is
shown in Figures 18 and 20. The difference was taken as the suboptimal
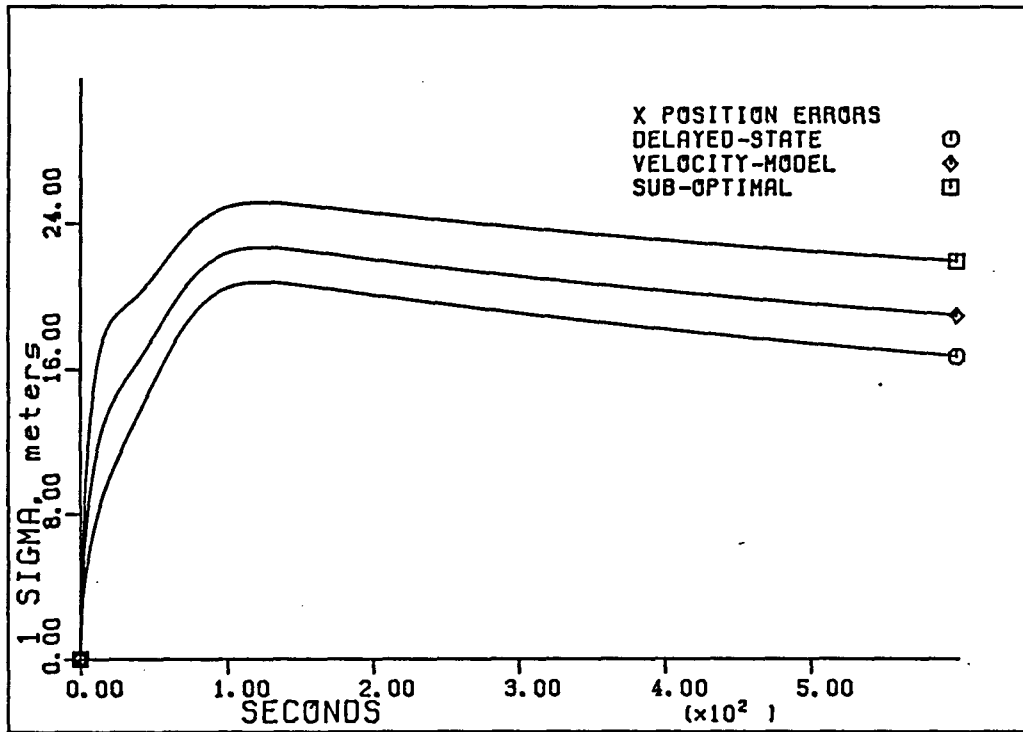
Figure 11.   x position error profiles for $\Delta t = 1s$
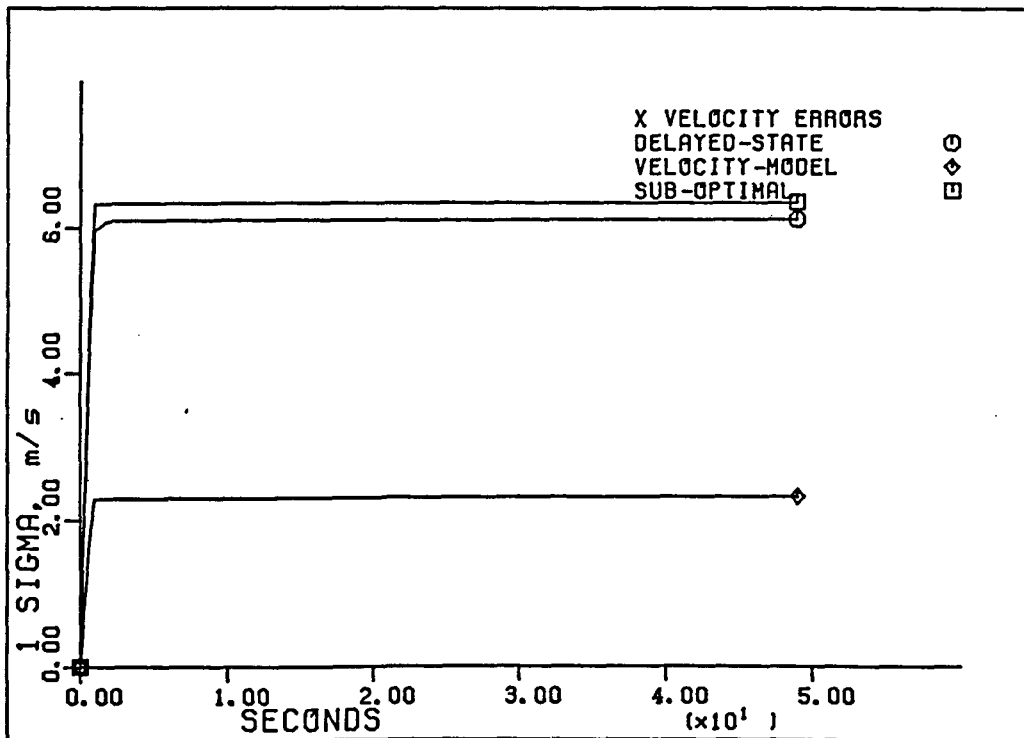
Figure 12.   x velocity error profiles for $\Delta t = 1s$
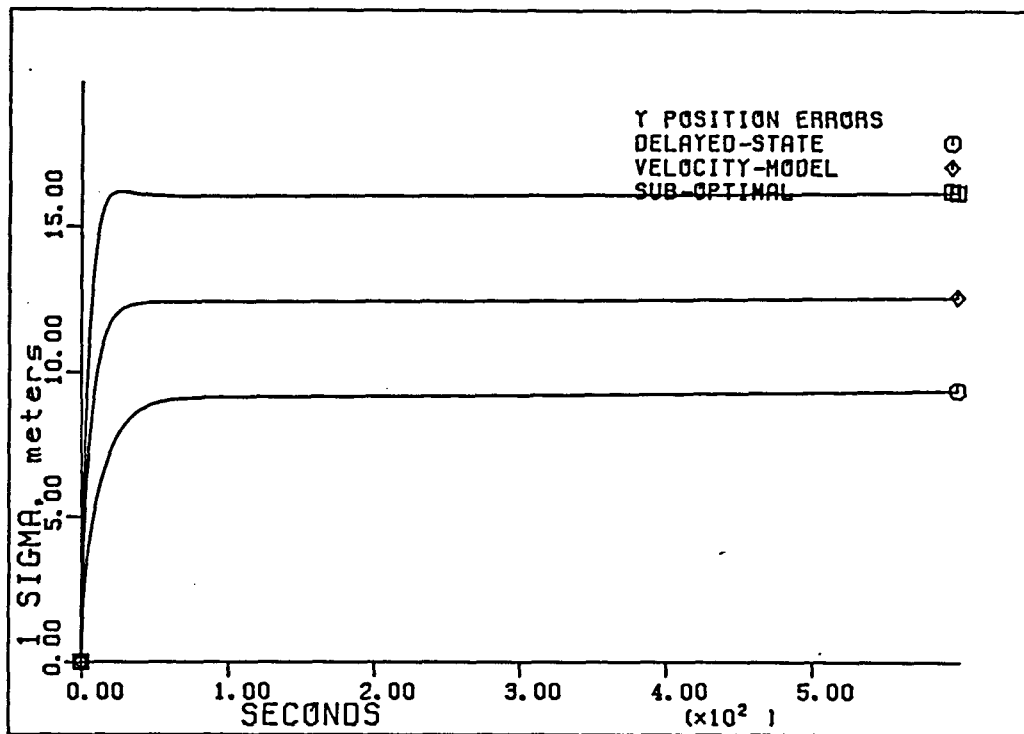
Figure 13. y position error profiles for $\Delta t = 1s$
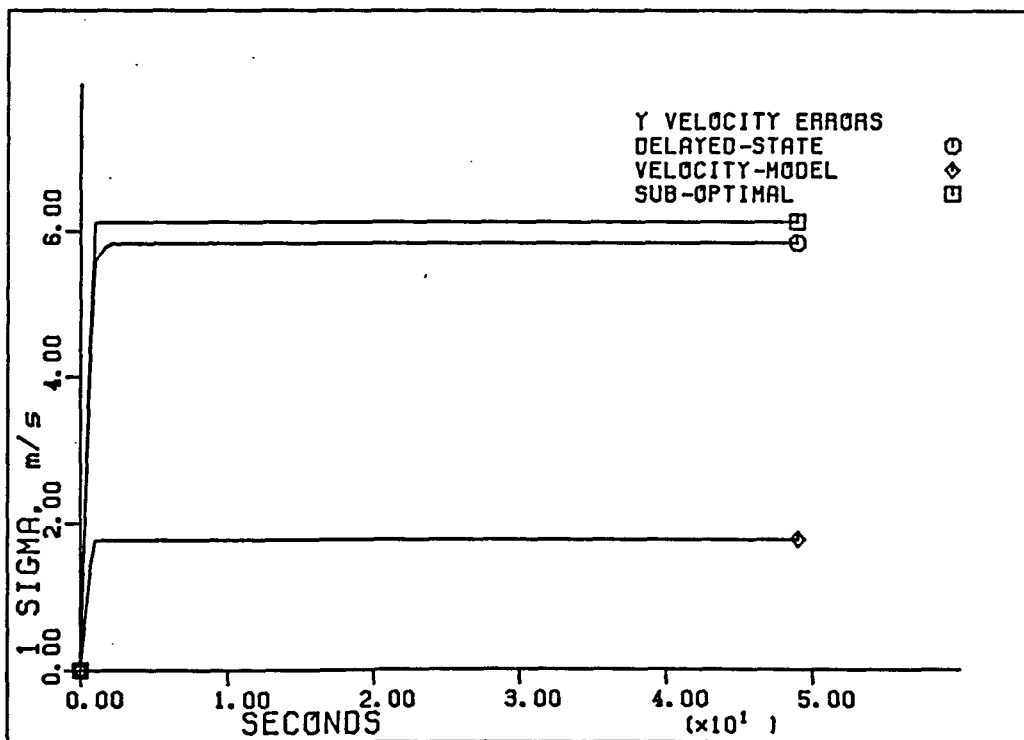
Figure 14. y velocity error profiles for $\Delta t = 1s$
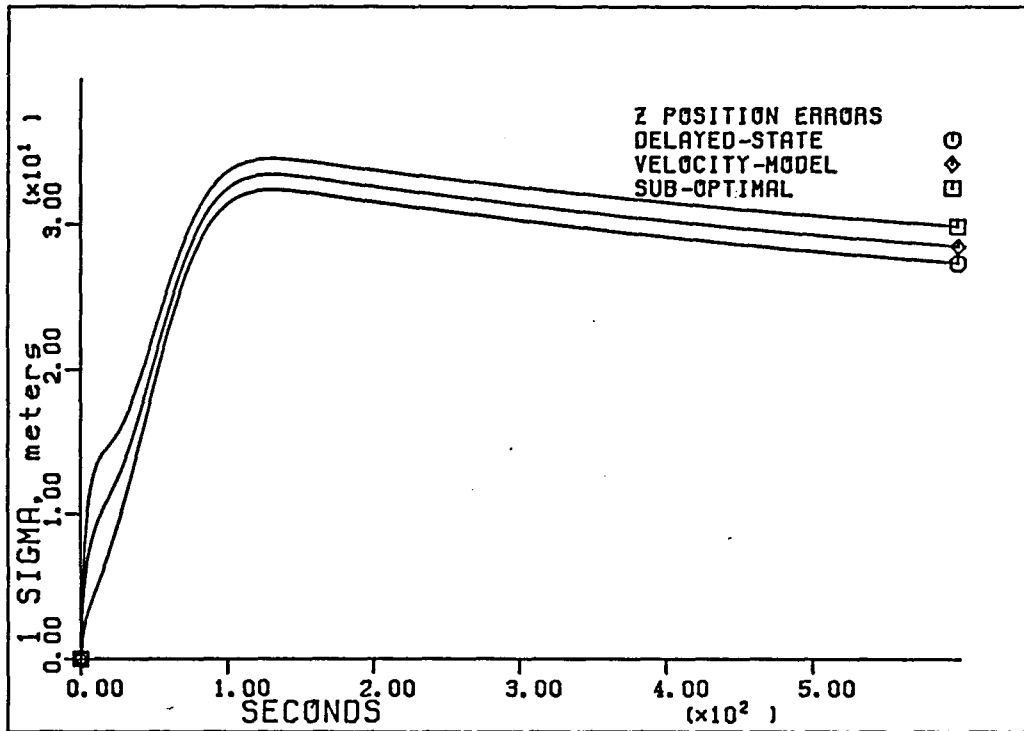
Figure 15.   z position error profiles for $\Delta t = 1s$
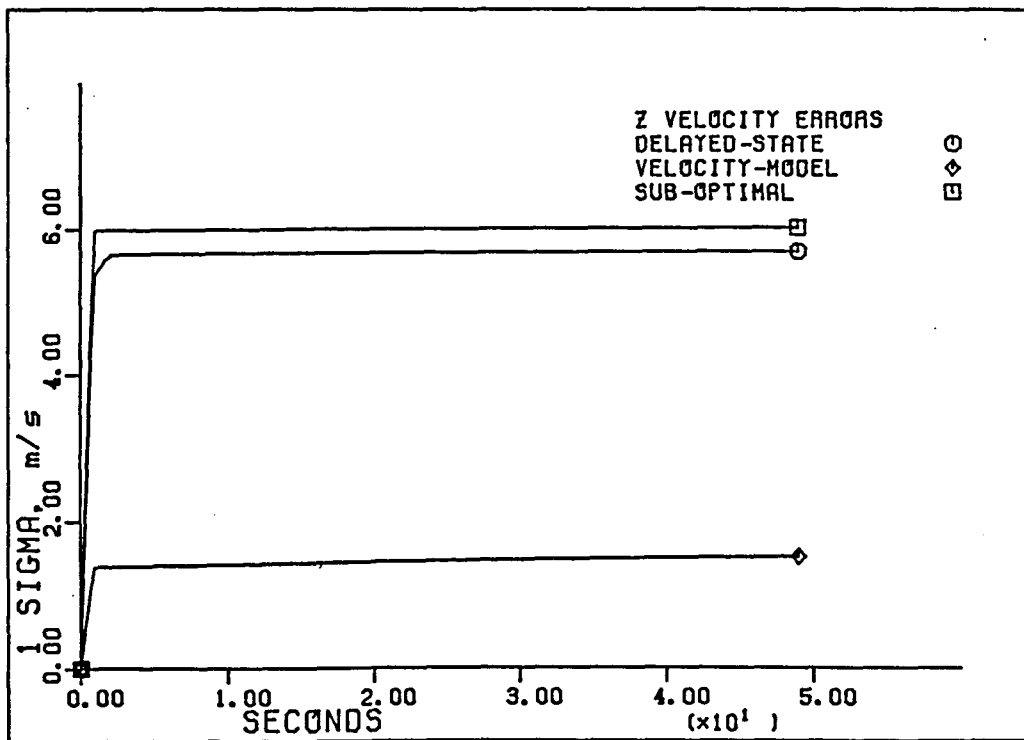
Figure 16.   z velocity error profiles for $\Delta t = 1s$
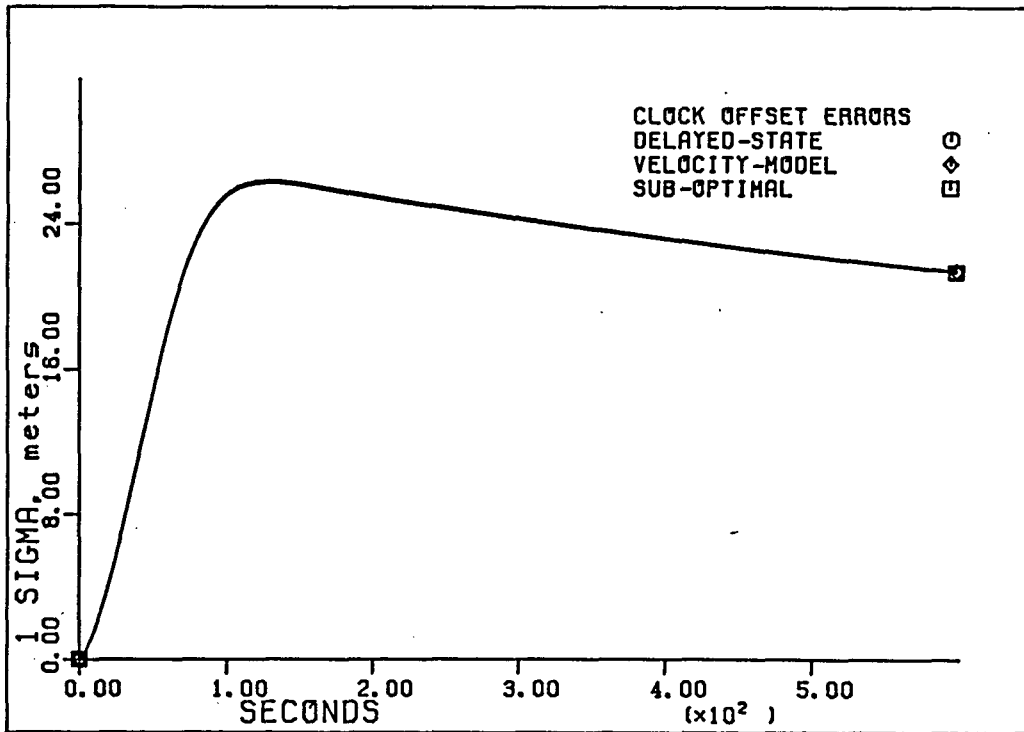
Figure 17.   Clock offset error profiles for $\Delta t = 1s$
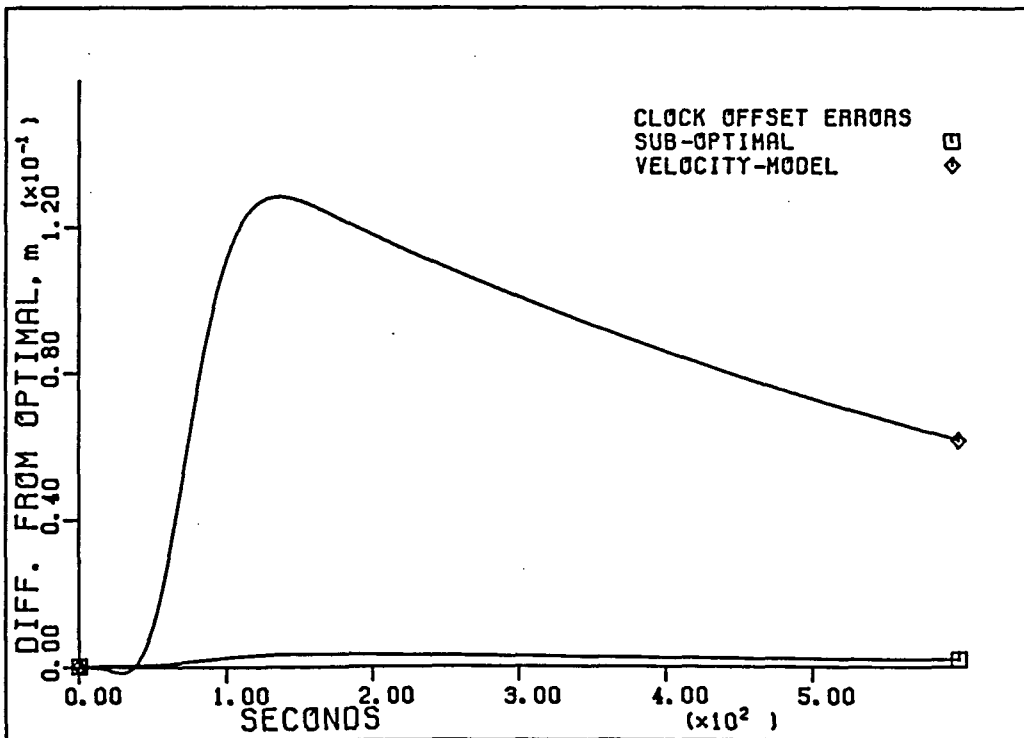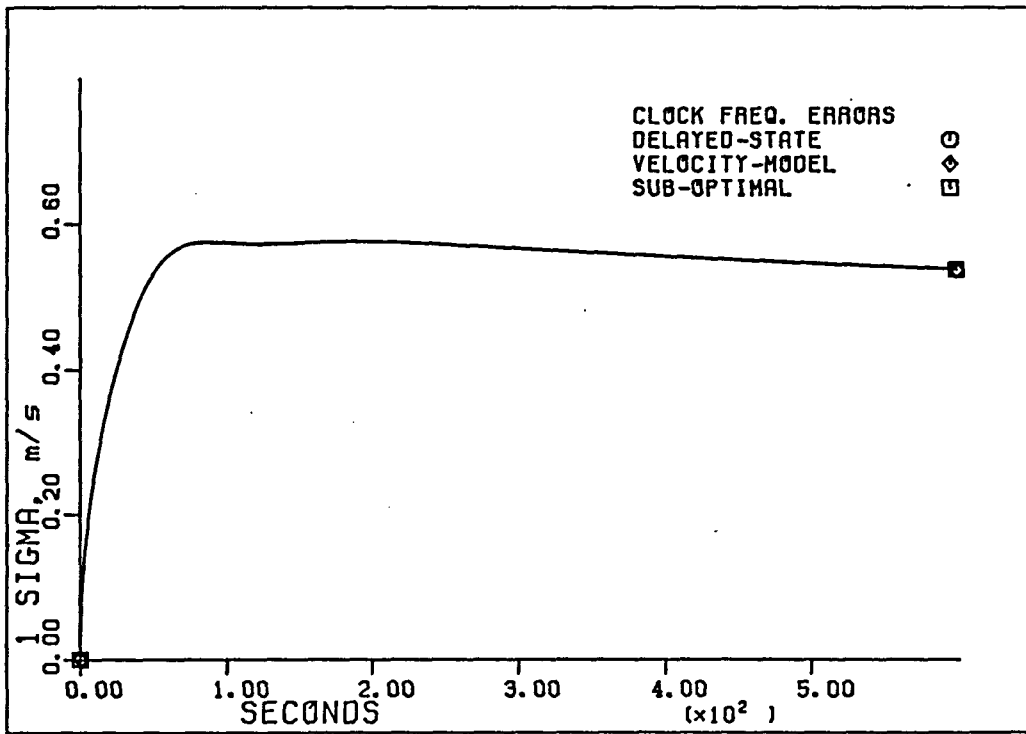

Figure 18.   Differences from the optimal offset error profile

Figure 19. Fractional frequency error profile for $\Delta t = 1s$
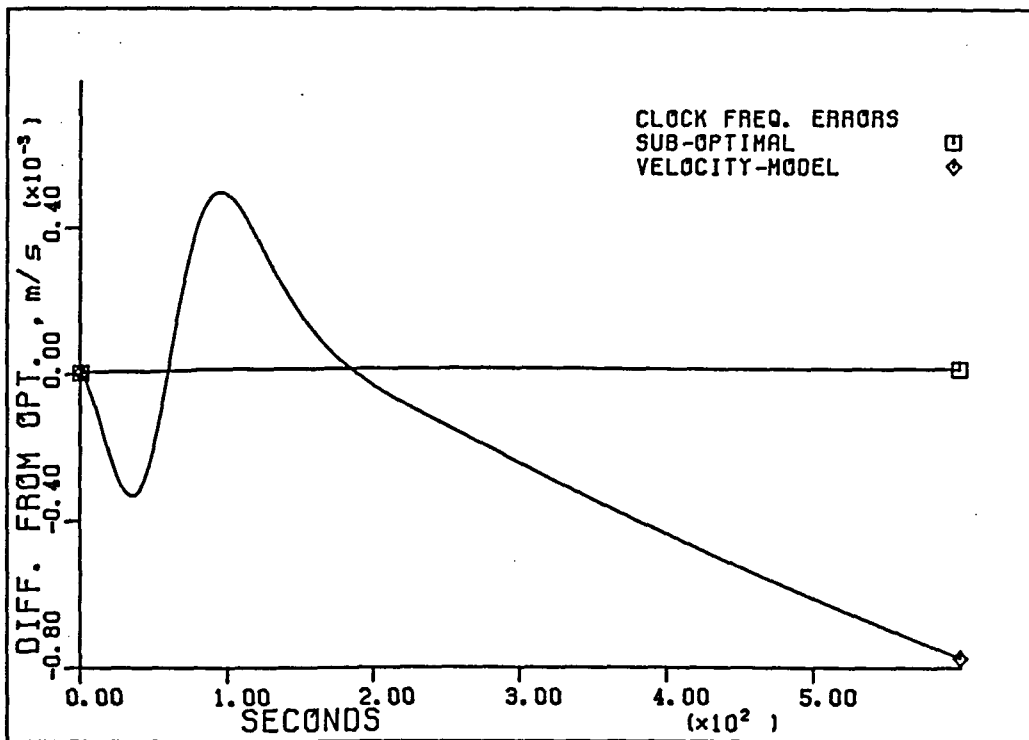
Figure 20. Differences from the optimal fractional frequency profile

less the optimal trajectory. The velocity model RMS clock errors vary about the optimal ones, as shown by the difference profile changing from positive to negative quantities. The RMS error trajectories calculated with the delayed state model using the suboptimal gains always remains greater than the optimal trajectories. In this case, the difference is small, but it always remains positive. The important observation is that the profiles of the RMS errors from the delayed state model using the suboptimal gains are always larger than the profiles obtained with the optimal gains in the delayed state filter. Of course, this result is expected because by definition, the Kalman gains are the gains which minimize the elements along the main diagonal of the error covariance matrix. Table 2 gives a summary of the steady state RMS error values for a one second sampling interval.

Table 2. Semi-steady state RMS errors

State	Baseline	Delayed state	Velocity model	Suboptimal
x pos.	45m	15m	18m	21m
x vel.	18m/s	6m/s	2.5m/s	6.5m/s
y pos.	32m	8.5m	12m	16m
y vel.	16m/s	5.8m	1.8m/s	6.2m/s
z pos.	42m	27m	29m	31m
z vel.	15m/s	5.6m/s	1.4m/s	6.0m/s
Clock offset	1m/s	22m	22m	22m
Clock fractional frequency	1m/s	.56m/s	.56m/s	.56m/s

The point to be made from all this is that the velocity model is a physically fictitious model, but mathematically it is a reasonable approximation to the delayed state model when the time interval between the phase difference measurements is small. The fact that the standard deviations of the velocity error states determined with the velocity model are smaller than those obtained with the delayed state model does not mean that the velocity model is superior. Rather, it is a result of a very optimistic assumption made in the very beginning of the derivation of the velocity model. The assumption that the Doppler shift is proportional to an instantaneous measurement of relative velocity is not physically reasonable.

The time interval between measurements was then decreased to one-tenth of a second to see if the velocity model would become a better approximation of the delayed state model. The standard deviation profiles determined with the velocity model, the delayed state model and the delayed state model with the suboptimal gains for each of the state variables are shown in Figures 21-36. Since the time interval was decreased, fewer data are averaged and there should be more uncertainty associated with the Doppler measurement. This explains the increase in the R matrix elements, which is described above. The change in the time interval was also accounted for in the state transition matrix, the Q matrix and the measurement connection matrices (in the velocity model). The power spectral densities of the process noise remain the same, but the correct amount of uncertainty that enters the system over this time interval due to the process noise is taken care of in the Q matrix.
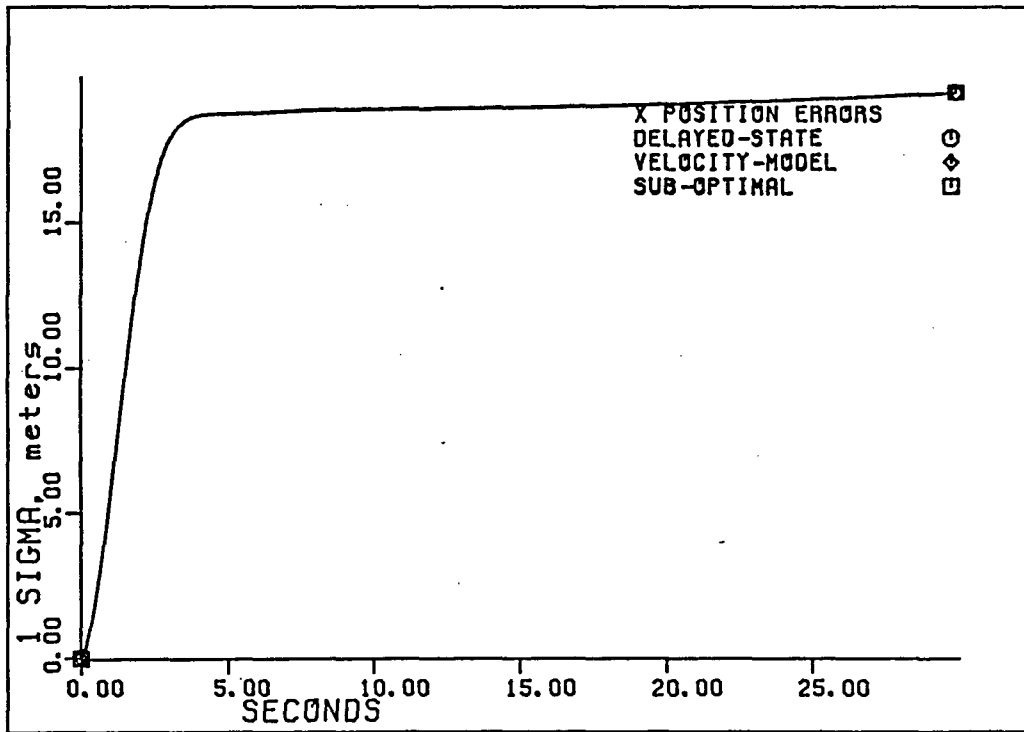
Figure 21. x position error profiles for Δt = .1s
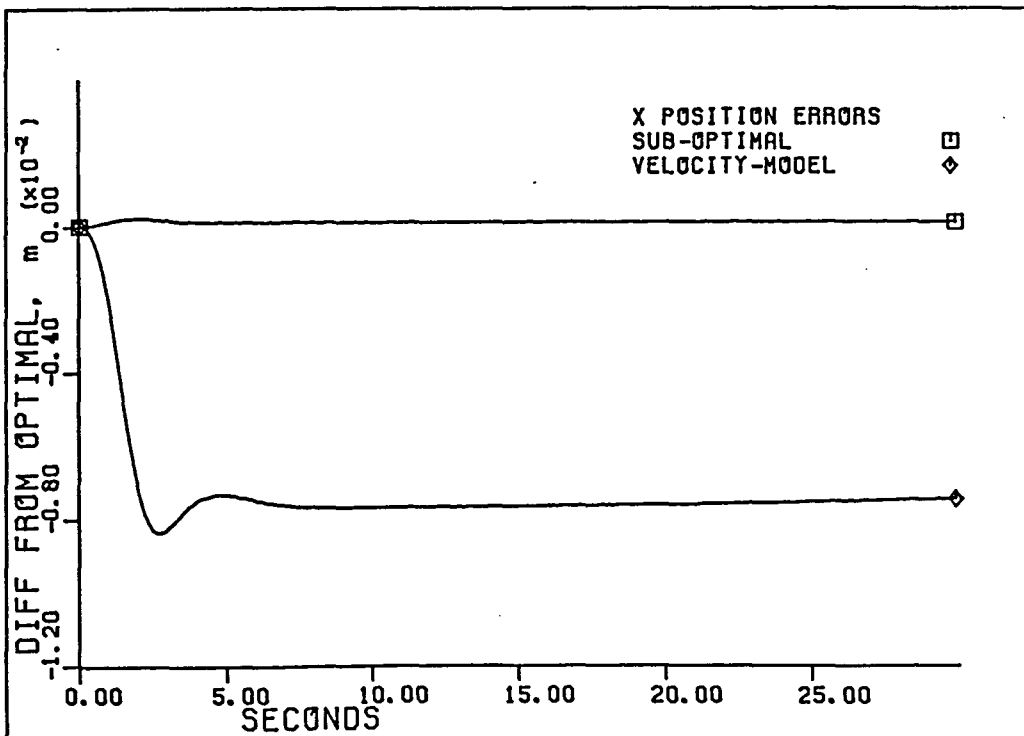
Figure 22. Differences from the optimal x position error profile
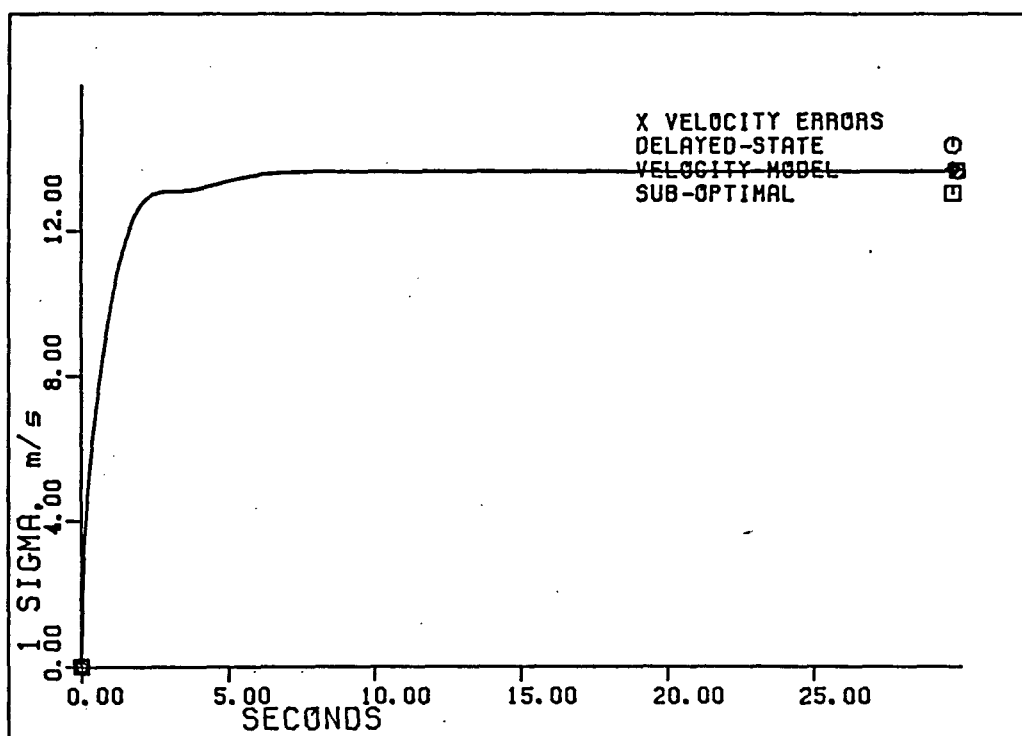
Figure 23.   x velocity error profiles for Δt = .1s
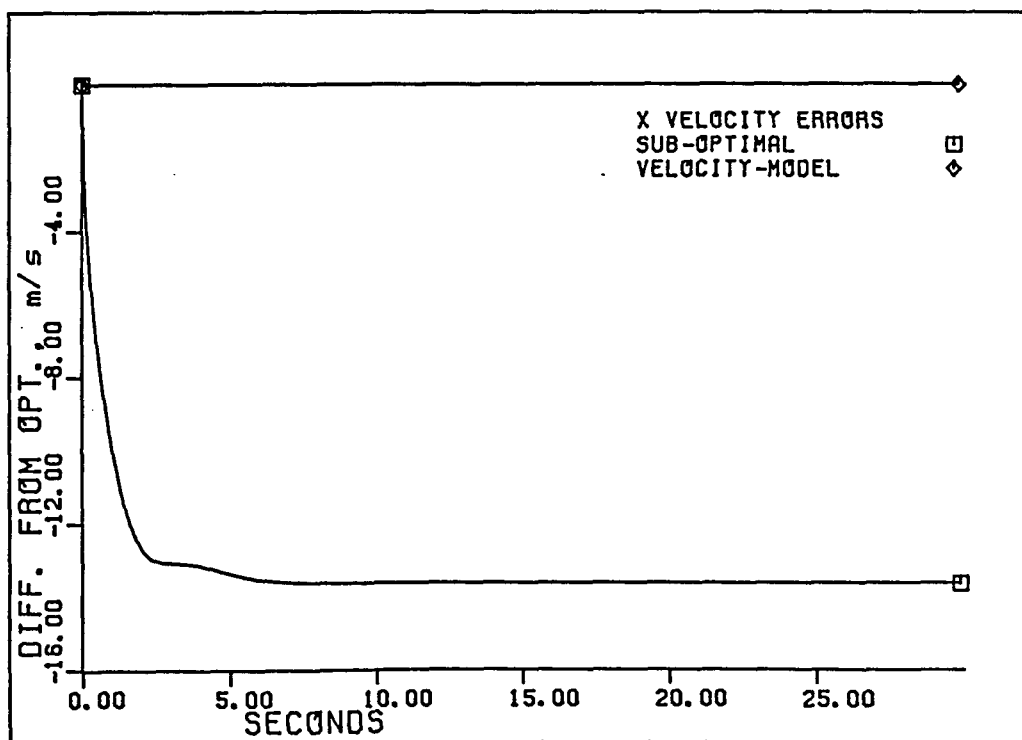

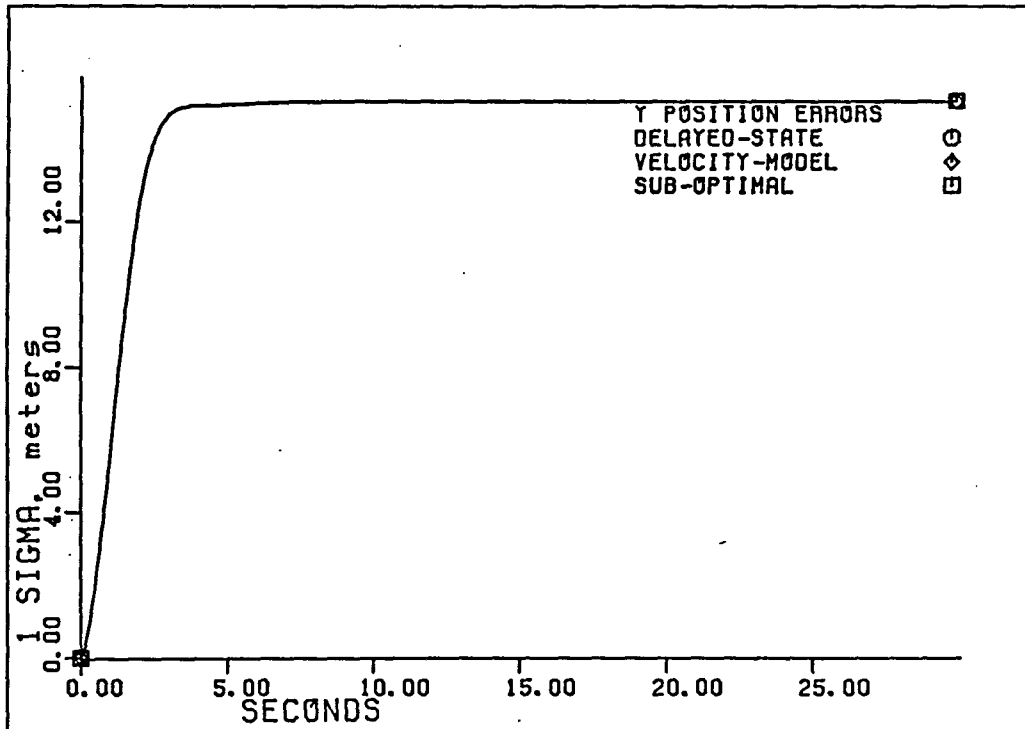Figure 24.   Differences from the optimal x velocity error profile
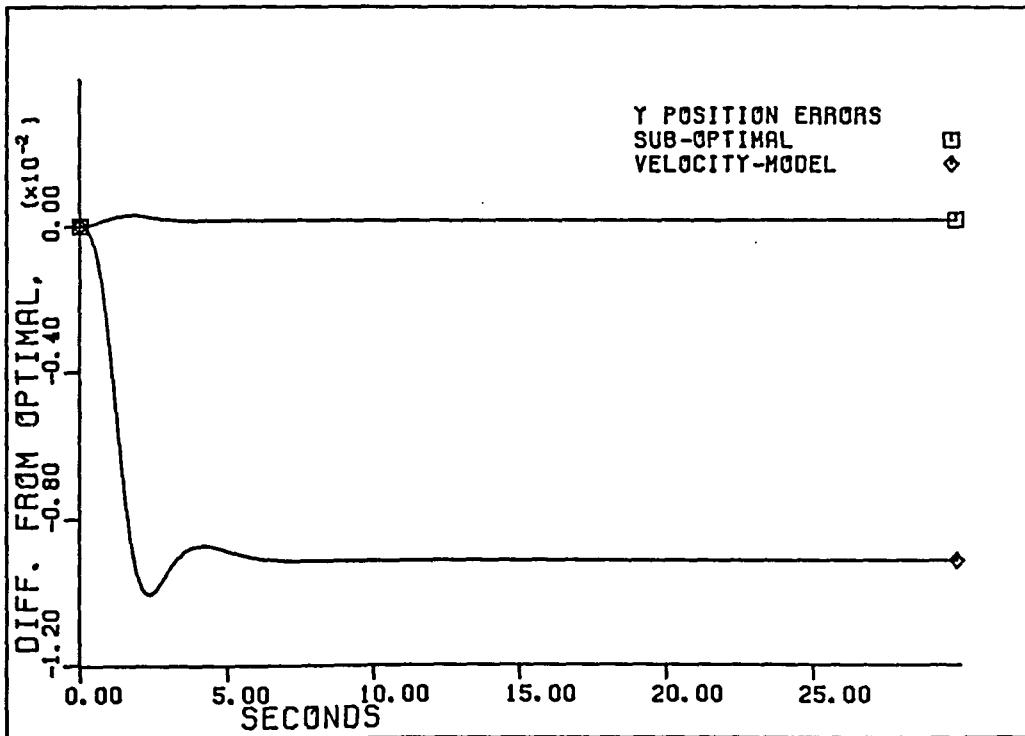
Figure 25. y position error profiles for Δt = .ls

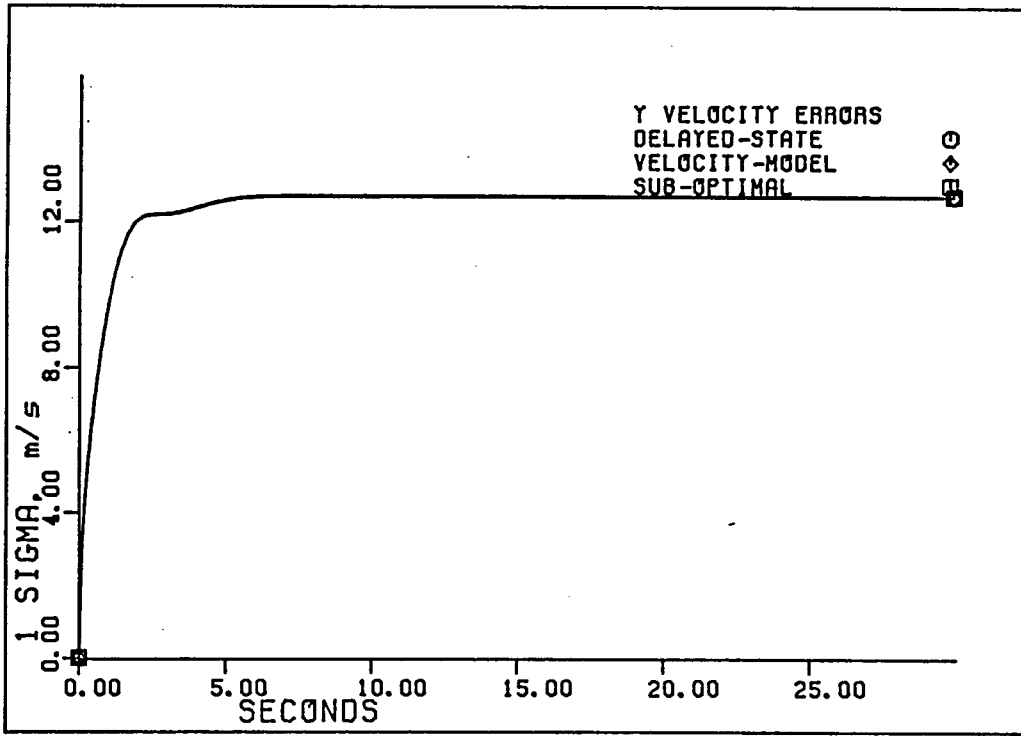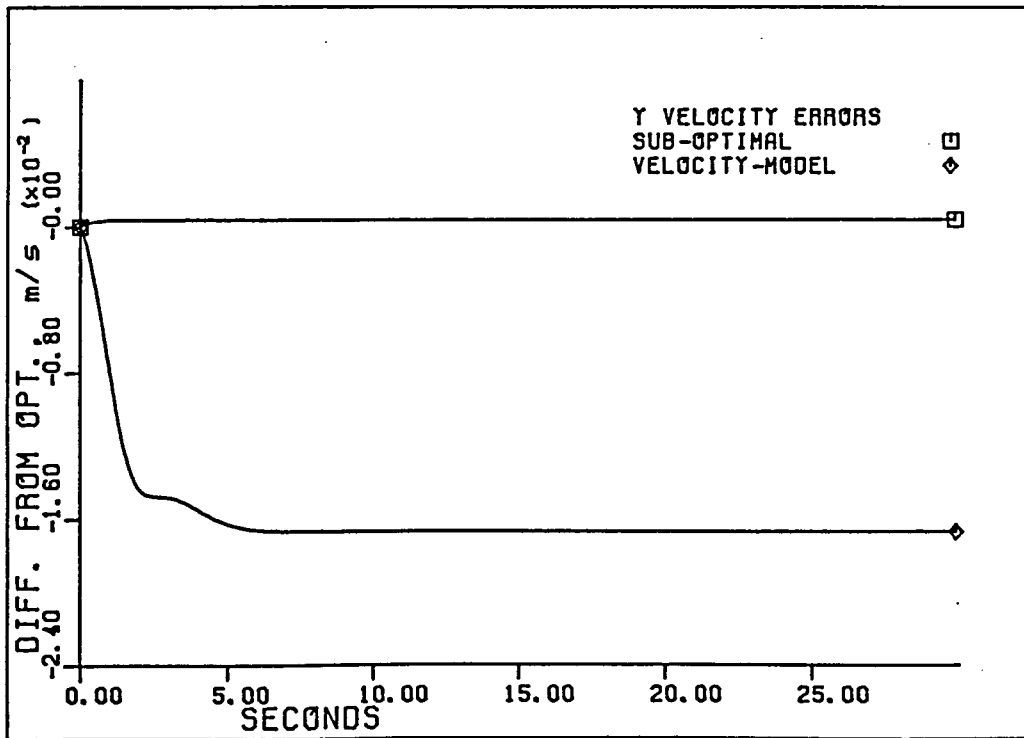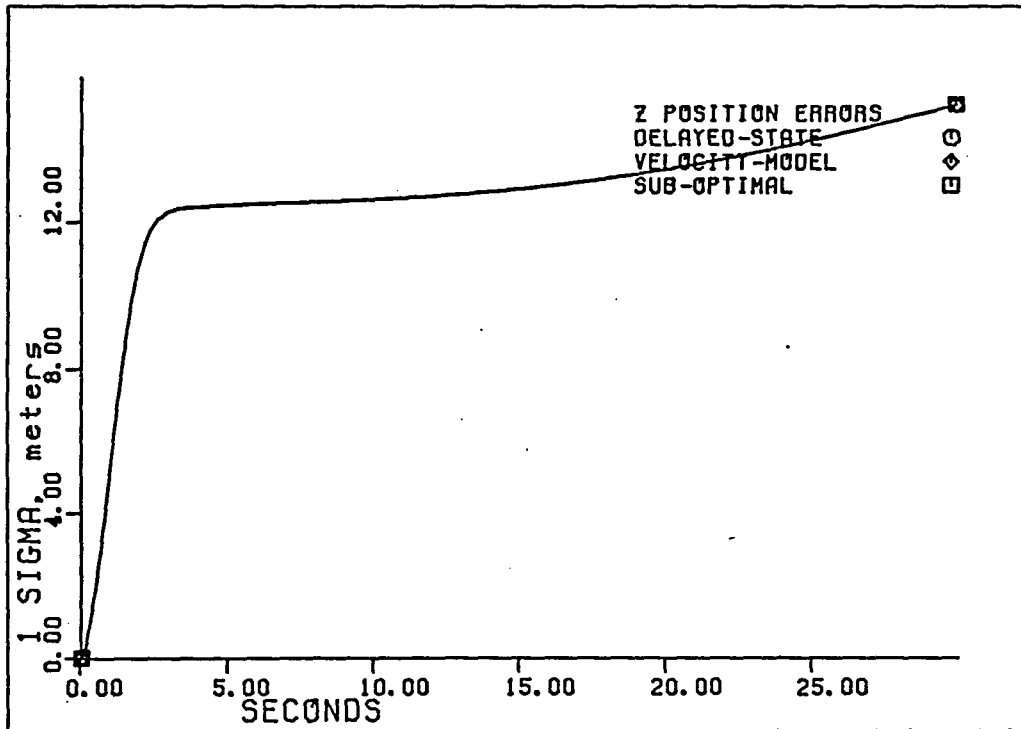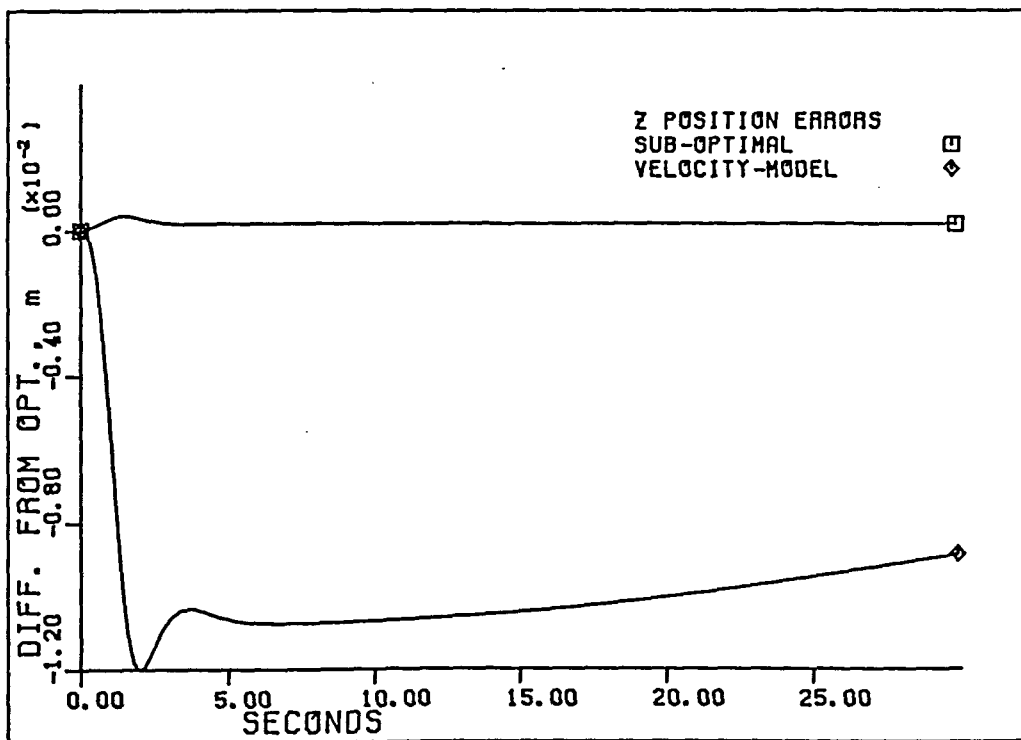Figure 26. Differences from the optimal y position error profile

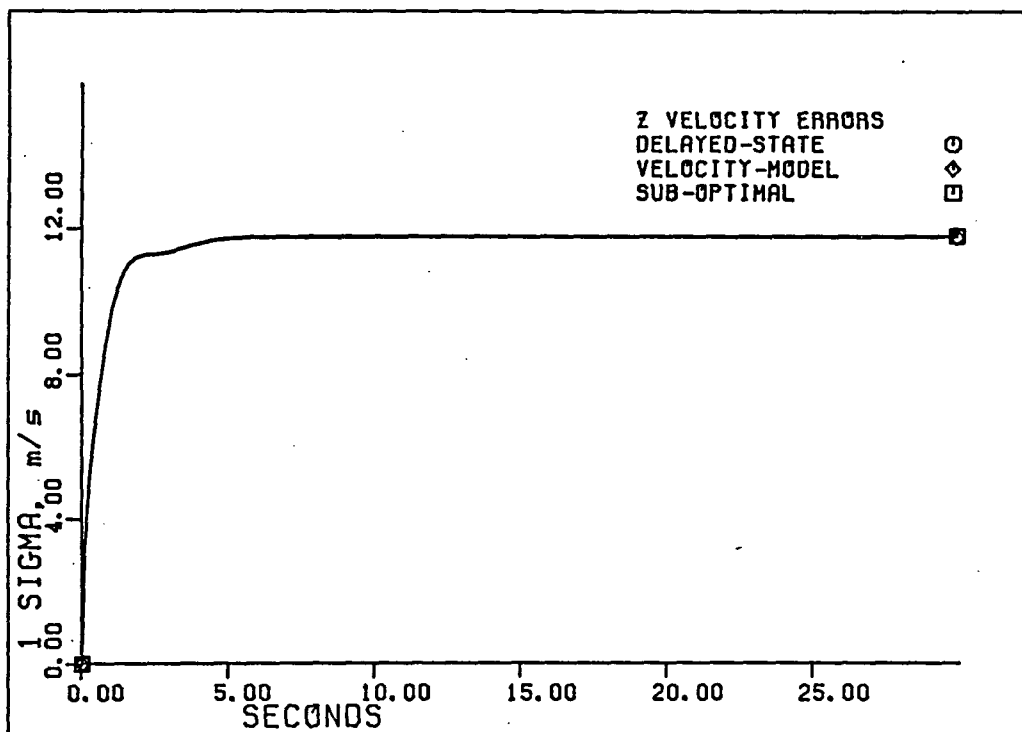Figure 27.   y velocity error profiles for Δt = .1s

Figure 28.   Differences from the optimal y velocity error profile

Figure 29.   z position error profiles for Δt = .1s

Figure 30.   Differences from the optimal z position error profile

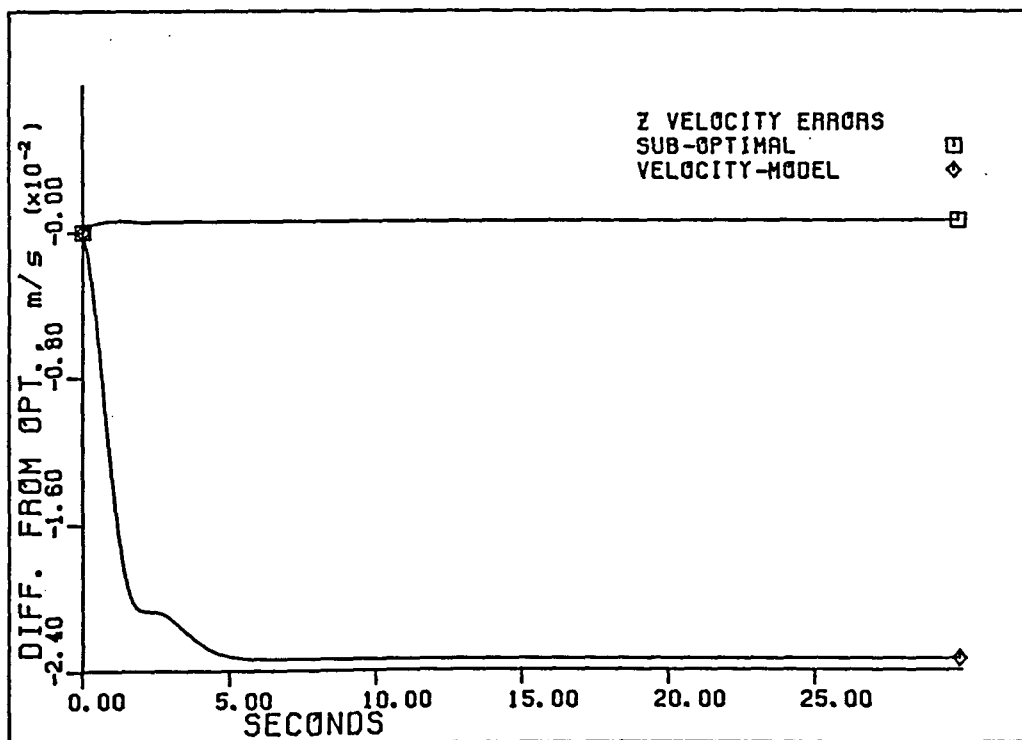Figure 31. z velocity error profiles for $\Delta t = .1s$

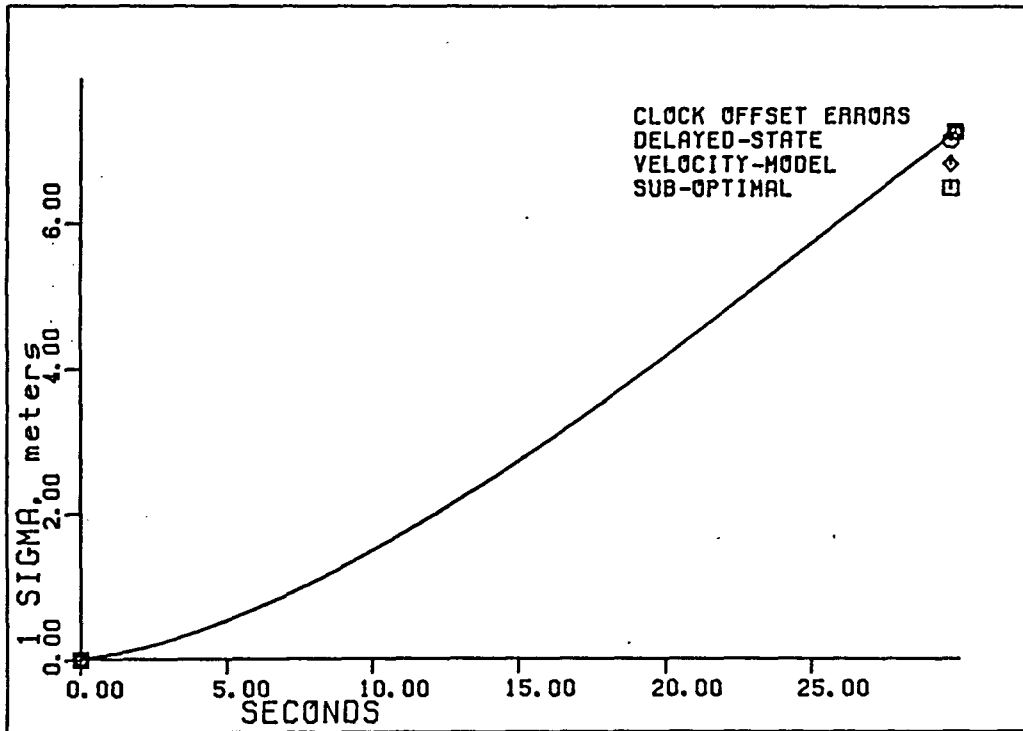Figure 32. Differences from the optimal z velocity error profile

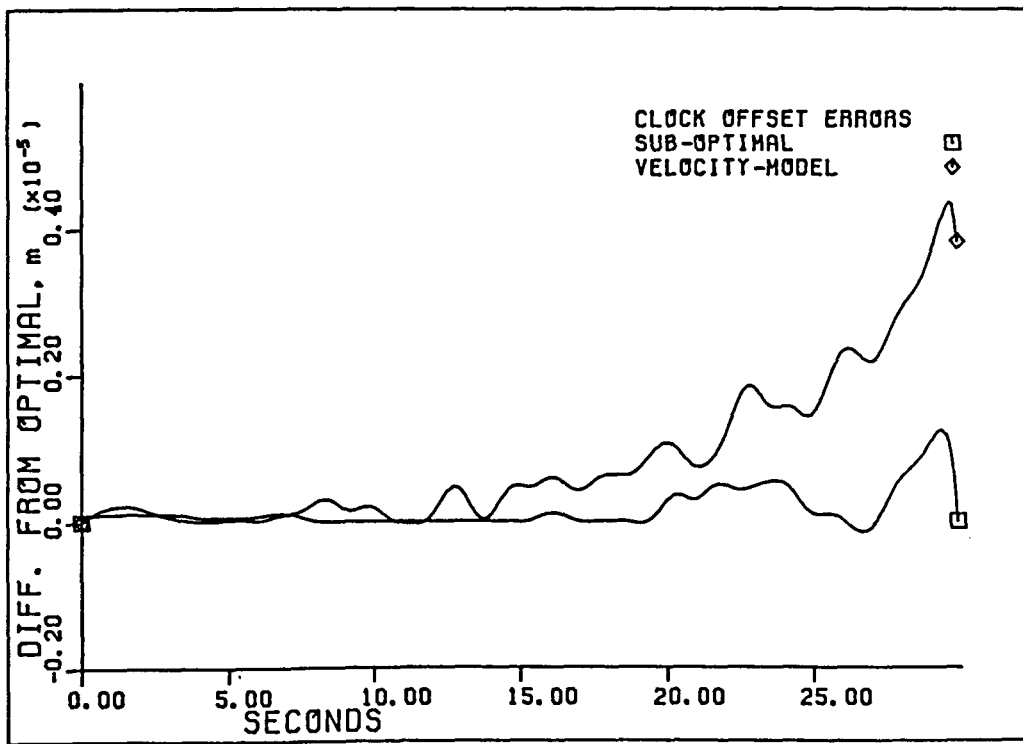Figure 33. Clock offset error profiles for Δt = .1s

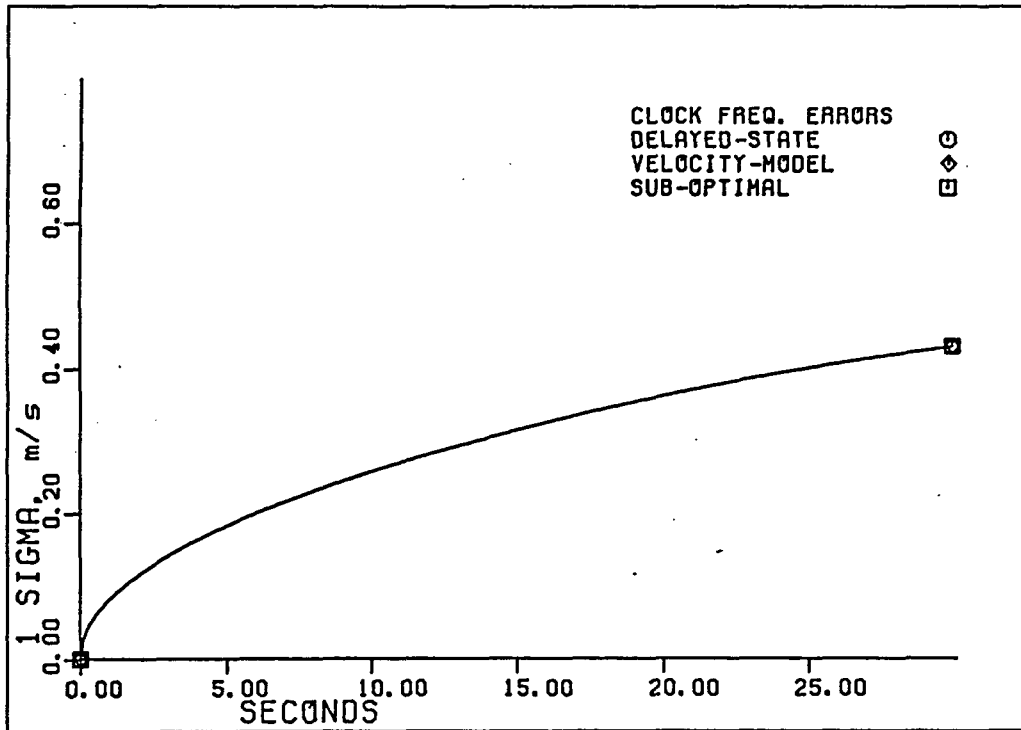Figure 34. Differences from the optimal offset error profile

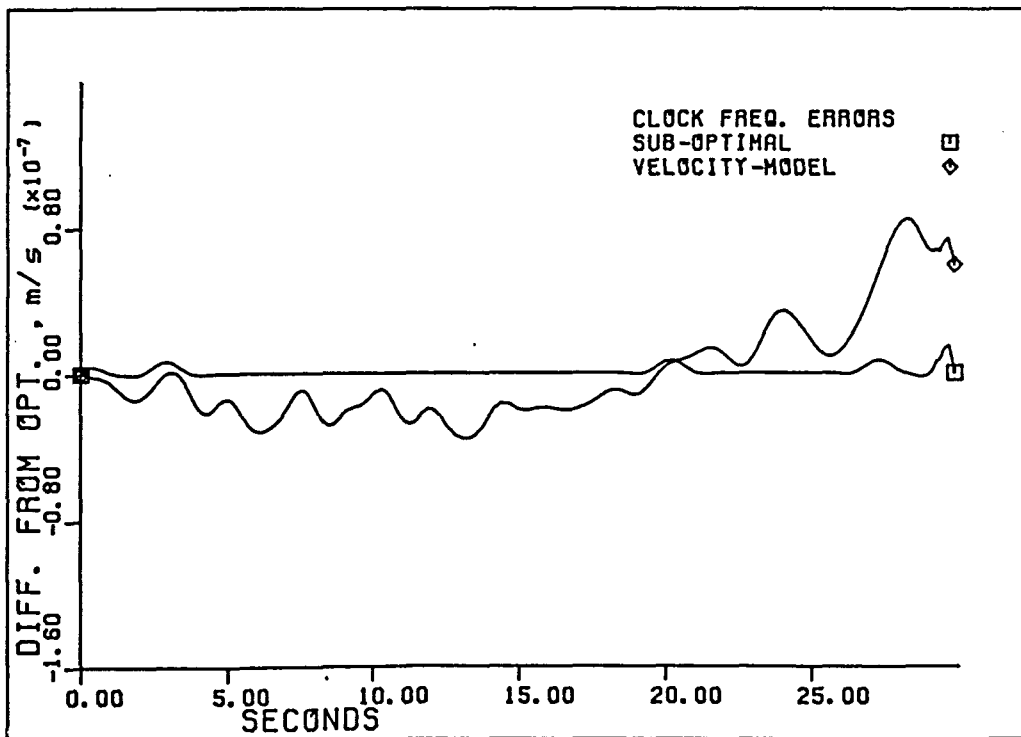Figure 35. Fractional frequency error profiles for $\Delta t = .1s$

Figure 36. Differences from the optimal fractional frequency error profile

The results are similar to those obtained when the time interval was one second. The standard deviations of the state variables obtained with the suboptimal gains are always slightly larger than those found with the optimal gains in the delayed state model. However, the difference is much less in this case. Once again, the difference in the standard deviation profiles from each of the three programs is too small to be observed from the plot. (This is because the plot scale is too large to show the difference.) For each of the state variables, the difference between the optimal profile and the other two profiles was plotted. Clearly, the difference between the velocity and the delayed state models has diminished as is expected. In all the velocity states, the velocity model predicted a smaller standard deviation than did the delayed state model and is shown by the difference between the two as being negative. This result is explained with the reasoning that the velocity model is a fictitious model and predicts overly optimistic statistics.

In all the clock error trajectories, it appears as though the standard deviations have not reached a steady state condition. However, the difference between the suboptimal and optimal trajectories always remains positive and there is no indication of any filter divergence problems. The difference was very small and quite erratic, and the plotting routine performed some smoothing to obtain the plots shown in Figures 34 and 36. This smoothing was not needed for all the other plots, though.

It should be mentioned that all the trajectories are obtained

from discrete type data and that interpolation was used to get the
continuous plots for Figures 9-36. The point to point interpolation
was performed by the plotting routine.

IV. CONCLUSION

It has been shown that the delayed state Kalman filter will allow for optimal processing of GPS carrier Doppler shift measurements. The need for the delayed state Kalman filter arises from the fact that the Doppler count measurement made with the GPS receiver is the integral of the Doppler shift over the interval that the phase difference measurement is made. When this measurement is linearized about a nominal trajectory, the Kalman filter measurement is related to present as well as previous (delayed) system errors. The presence of the delayed state in the measurement equation cannot be accommodated with the usual Kalman filter measurement equation. To get around this problem, another term is added onto the Kalman filter measurement equation which accounts for the connection of the current measurement to the previous state. The result is the delayed state Kalman filter and the corresponding recursive equations.

The error covariance of the random process being estimated (in this case the system errors) with the Kalman filter may be computed without actual measurement data. This provides the filter designer with a powerful indicator of the range of accuracy to be expected (for the system as it is modelled) without having to perform time consuming Monte Carlo type simulations. If less than optimal gains are cycled through the Kalman filter, the resulting error variances should be greater than those obtained with the Kalman gains. Thus, gains from a model considered to be an approximation to the truth model can be

cycled through the truth model's error covariance update equation to determine the relative accuracy of the approximate model. This method is known as suboptimal error analysis. It is also referred to in this research as suboptimal gain substitution.

Suboptimal error analysis techniques were used to compare the true measurement model (where the Doppler count is the integral of the Doppler shift) to a model that considers the Doppler count measurement as proportional to an instantaneous frequency measurement. The latter type of measurement does not make physical sense even though mathematically this model can be shown to be an approximation to the true model in the limit as the time over which the phase difference measurement is performed tends toward zero. The results obtained for the relative difference of the system RMS error profile between the optimal and suboptimal filters were not larger than a few meters in the position states for an integration interval of one second. However, this is enough difference to show that delayed state model developed, and the use of the delayed state Kalman filter to process the Doppler count measurements, will be optimal with respect to other approximate models. (Some degree of suboptimallity enters the problem by linearizing the measurement equation since the Kalman filter demands a linear measurement equation.) The really important difference between the delayed state model (which gives the true RMS error) and the fictitious velocity model shows up mainly in the velocity estimation errors. In this case, the velocity model predicts unduly optimistic results. This gives an indication of the crudeness of the velocity model as an approximation

to the delayed state model. The degree of increased numerical com-
plexity in the delayed state Kalman filter recursive equations is quite
manageable and worthwhile in the sense that the real life improvement
in using this model may be significant.

This research was not intended to determine the absolute accuracy
of a typical state-of-the-art aided INS. A rather crude inertial system
was modelled with the choices of the white noise power spectral densi-
ties that drive the process state equation. The amplitudes that were
used led to INS velocity errors of ten meters per second and INS posi-
tion errors of six meters over a one second sampling interval. Clearly,
a state-of-the-art inertial system would not be in error to this extent
over such an interval. Also, the measurement error associated with the
pseudo-range and delta-range measurements were chosen to be large with
respect to current technology. A common pseudo-range measurement error
might be twenty meters. This is more than a factor of two smaller
than the fifty meter error assumed for this research. The large
measurement and process errors were used simply to help demonstrate the
difference between the two different models.

If the absolute accuracy of an aided INS using the best available
inertial system and GPS receiver was desired, models could have been
developed which are much more complicated but could account for specific
aspects of a real aided INS. For example, the statistics of the actual
measurement noise (obtained using a specific GPS receiver) might be
empirically determined to be a colored noise process rather than purely
white. Also, the errors of a specific accelerometer or gyro could be

modelled to fit empirical data and would lead to a different process model than pure double integration. The corresponding Kalman filter states would be augmented to account for these specifics. In this case, it would be possible to compare absolute accuracy between the delayed state and velocity models when suboptimal error covariance analysis is performed. This type of analysis is not really needed if only the relative accuracy is desired. Even though the model used in this research is rather general, it is justified because it accounts for the dominant system errors and is fairly representative of a typical aided INS.

V. REFERENCES

1. Brown, A.; Matthews, T.; and Varty, T. "Low Cost Testing of a High Accuracy INS Using GPS." The Institute of Navigation, Proc. of the National Technical Meeting (Addendum, pp. 24-29). Washington, D.C.: Institute of Navigation, 1986.

2. Brown, R. G. "Integrated Navigation Systems and Kalman Filtering: A Perspective." Navigation, J. Inst. Navigation 19, No. 4 (Winter 1972-73):355-362.

3. Brown, R. G. Introduction to Random Signal Analysis and Kalman Filtering. New York: John Wiley & Sons, 1983.

4. Brown, R. G.; and Hagerman, L. L. "An Optimum Inertial/Doppler Satellite Navigation System." Navigation, J. Inst. Navigation 16, No. 3 (Fall 1969):260-296.

5. Brown, R. G.; and Hartman, G. L. "Kalman Filter with Delayed States As Observables." Proc. of the National Electronics Conference 24 (1968):67-72.

6. Copps, E. M.; Geier, G. J.; Fidler, W. C.; and Grundy, P. A. "Optimal Processing of GPS Signals." Navigation, J. Inst. Navigation 27, No. 3 (Fall 1980):171-182.

7. Denaro, R. P. "NAVSTAR Global Positioning System Offers Unprecedented Navigation Accuracy." Microwave System News 14, No. 12 (November, 1984):54-83.

8. Eschenback, R.; and Helkey, R. "Performance/Cost Ratio Optimized for GPS Receiver Design." Microwave System News 14, No. 12 (November, 1984):43-52.

9. Parkinson, B. W.; and Gilbert, S. W. "NAVSTAR: Global Positioning System--Ten Years Later." Proc. of the IEEE 71, No. 10 (October, 1983):1177-1186.

10. Van Dierendonk, A. J.; McGraw, J. B.; and Brown, R. G. "Relationship Between Allan Variances and Kalman Filter Parameters." Proceedings of the Sixteenth Annual Precise Time and Time Interval (PTTI) Applications and Planning Meeting, Greenbelt, Maryland, November 1984.

VI.   ACKNOWLEDGMENTS

I would like to thank my major professor Dr. R. Grover Brown for the motivation he provided for this research. He has provided invaluable guidance, insight, direction, and support throughout the completion of this project.

Appreciation and thanks should be extended to Dr. Larry Coady and Dr. Ken Heimes for their willingness to serve on my graduate committee.

I would also like to express my appreciation to my parents and Dr. Kuo Ho Yang for the motivation they gave me to pursue my graduate education.

Finally, I wish to thank my typist Carolyn Taylor for the excellent work she provided.

VII. APPENDIX A. APPROXIMATION OF THE
DELAYED STATE MODEL

The velocity model assumes a physically unrealistic measurement situation, but this model may be shown mathematically to be an approximation to the delayed state model. The approximation becomes valid as the time between the phase measurements, used to measure Doppler count, tend towards zero. To show this, the mean value theorem of calculus will be invoked. The theorem states that if a function $f(x)$ is continuous on the closed interval $[a,b]$ and if $f(x)$ is differentiable on the open interval (a,b), then there is a value of the independent variable c, contained in (a,b), such that:

$$\dot{f}(c) = [f(b) - f(a)]/(b-a) \tag{51}$$

Let the time between t_{n-1} and t_n be Δt. Let c_1 be contained in the interval t_{n-1} to $t_n - \Delta t/2$. Then, using 51:

$$f(t_{n-1}) = f(t_n - \Delta t/2) - \Delta t/2 \; \dot{f}(c_1) \tag{52}$$

Let c_2 be contained in the interval $t_n - \Delta t/2$ to t_n. Also, by 51 the following is true:

$$f(t_n) = f(t_n - \Delta t/2) + \Delta t/2 \; \dot{f}(c_2) \tag{53}$$

Since the cosine function satisfies the continuity and differentiability criteria stated above, the mean value theorem can be invoked to write:

$$\cos\theta(t_{n-1}) = \cos\theta(t_n - \Delta t/2) - \Delta t/2 \ \Delta\cos\theta(c_1) \qquad (54)$$

$$\cos\theta(t_n) = \cos (t_n - \Delta t/2) + \Delta t/2 \ \Delta\cos\theta(c_2) \qquad (55)$$

where $\Delta\cos\theta(a)$: time differential change in $\cos\theta(t)$ at $t=a$

Applying equations 54 and 55 to the delayed state measurement equation 14 and collecting terms, the result is:

$$
\begin{aligned}
z - h(t_n) = -f_0/c[&-\cos\theta_{x\rho}(t_n - t/2)\{\Delta x(t_n) - \Delta x(t_{n-1})\} \\
&- \cos\theta_{y\rho}(t_n - t/2)\{\Delta y(t_n) - \Delta y(t_{n-1})\} \\
&- \cos\theta_{z\rho}(t_n - t/2)\{\Delta z(t_n) - \Delta z(t_{n-1})\} \\
&+ c\{\Delta T(t_n) - \Delta T(t_{n-1})\} - \Delta t/2\{\Delta\cos\theta_{x\rho}(c_1)\Delta x(t_n) \\
&+ \Delta\cos\theta_{x\rho}(c_2)\Delta x(t_{n-1})\} - \Delta t/2\{\Delta\cos\theta_{y\rho}(c_1)\Delta y(t_n) \\
&+ \Delta\cos\theta_{y\rho}(c_2)\Delta y(t_{n-1})\} - \Delta t/2\{\Delta\cos\theta_{z\rho}(c_1)\Delta z(t_n) \\
&+ \Delta\cos\theta_{z\rho}(c_2)\Delta z(t_{n-1})\}] + v(t) \qquad (56)
\end{aligned}
$$

By dividing both sides of equation 56 by Δt where Δt gets very small, and by noting that the last three terms inside the brackets will be second order differences, and thus can be ignored as Δt tends toward zero, equation 56 becomes:

$$
\begin{aligned}
z - h(t_n) = -f_0/c[&-\cos\theta_{x\rho}(t_n)\Delta\dot{x}(t_n) - \cos\theta_{y\rho}(t_n)\Delta\dot{y}(t) \\
&- \cos\theta_{z\rho}(t_n)\Delta\dot{z}(t_n) + c\Delta\dot{T}(t_n)] + v(t) \qquad (57)
\end{aligned}
$$

where $\Delta\dot{x}(t_n) = [\Delta x(t) - \Delta x(t_{n-1})]/\Delta t$ as Δt tends to zero and
similarly for $\Delta\dot{y}$, $\Delta\dot{z}$, and $\Delta\dot{T}$.

Here, it has been shown that the velocity model is a reasonable

mathematical approximation to the delayed state model if the phase

difference measurement interval is very small.

VIII.   APPENDIX B.   DERIVATION OF SATELLITE
DIRECTION COSINES

The following is the derivation of the direction cosines which are used to load the time varying measurement equation connection matrices. The procedure used here assumes a spherical satellite orbit so this method is only good for a computer simulation type study. In a real GPS receiver, the satellite ephemeris information is decoded to provide satellite positioning data in a given frame. Still, the general procedure is somewhat similar for producing the direction cosines. The satellite and vehicle coordinates must be brought into the same coordinate frame so that the vector from the vehicle to the satellite may be found. When the components of this vector are known, the direction cosines are easily obtained. Any suitable coordinate frame would be acceptable, but here it has been chosen to bring the satellite coordinates into a locally level earth fixed frame (x,y,z) where x is north, y is west and z is radially upward. The vehicle coordinates in this earth centered inertial frame of reference are:

$$R_v = 0\ \hat{i}_x + 0\ \hat{i}_y + R_v\hat{i}_z \tag{58}$$

where $\hat{i}_n$: unit vector in the n direction

To bring the satellite position vector into this frame, the satellite will initially be defined in its own earth centered inertial frame (U,V,W). The satellite position is then defined as:

$$\mathbf{R}_s = 0\ \hat{i}_U + 0\ \hat{i}_V + R_s\hat{i}_W \tag{59}$$

The satellite vector may be brought into an earth centered earth fixed (ECEF) coordinate frame (X,Y,Z) under the transformation:

$$R_{s_{X,Y,Z}} = T_1 \, R_{s_{U,V,W}} \tag{60}$$

The T_1 matrix is a transformation matrix which contains the direction cosines between the X,Y,Z unit vectors and the U,V,W unit vectors. By taking advantage of the sparsity of the vector in equation 59, R_s becomes:

$$R_{s_{X,Y,Z}} = R_{s_X} \hat{i}_X + R_{s_Y} \hat{i}_Y + R_{s_Z} \hat{i}_Z \tag{61}$$

where

$$R_{s_X} = R_s \cos\theta_{XW}$$
$$R_{s_Y} = R_s \cos\theta_{YW}$$
$$R_{s_Z} = R_s \cos\theta_{ZW}$$

where θ_{ab} refers to the angle between the a and b directions.

Using Figure 37 and performing a series of coordinate rotations
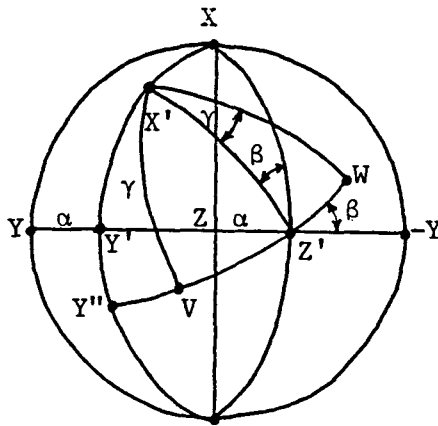
Figure 37. Transformation to ECEF coordinates

through the angles α, β, and γ, and by using the spherical law of
cosines, it is possible to find each of the components of equation
61. The angle α corresponds to angle of the ascending node which
is the longitude where the satellite orbit crosses the equator. The
angle β corresponds to the inclination angle which is the angle between
the orbit and the equator. The angle γ gives the angle of the
satellite along its orbit with respect to the ascending node.

The spherical law of cosines is given as (using Figure 38):

$$\cos a = \cos b \cos c + \sin b \sin c \cos A \tag{62}$$
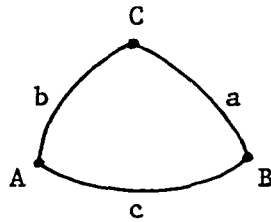
Figure 38. Spherical angles

Using Figure 37, the following direction cosines are found:

$$\cos\theta_{XW} = \cos\gamma \cos 90 + \sin\gamma \sin 90 \cos (90-\beta)$$
$$= \sin\gamma \sin\beta \tag{63}$$

$$\cos\theta_{YW} = \cos\gamma \cos(90+\alpha) + \sin\gamma \ \sin(90+\alpha)\cos(180-\beta)$$
$$= -\cos\gamma \sin\alpha - \sin\gamma \cos\alpha \cos\beta \tag{64}$$
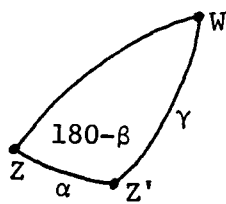
$$\cos\theta_{ZW} = \cos\alpha\ \cos\gamma + \sin\alpha\ \sin\gamma\ \cos(180-\beta)$$

$$= \cos\alpha\ \cos\gamma - \sin\alpha\ \sin\gamma\ \cos\beta \qquad (65)$$

The next step is to convert the satellite coordinates into the vehicle x,y,z coordinate frame. An arbitrary point in the ECEF frame is chosen and a series of coordinate rotations are performed to define the x,y,z frame. The angle ϕ corresponds to the vehicle east longitude and the angle θ corresponds to the vehicle north latitude. The new transformation is defined as:

$$R_{s_{x,y,z}} = T_2\ R_{s_{X,Y,Z}} \qquad (66)$$

$$\text{where}: T_2 = \begin{bmatrix} \cos\theta_{xX} & \cos\theta_{xY} & \cos\theta_{xZ} \\ \cos\theta_{yX} & \cos\theta_{yY} & \cos\theta_{yZ} \\ \cos\theta_{zX} & \cos\theta_{zY} & \cos\theta_{zZ} \end{bmatrix}$$

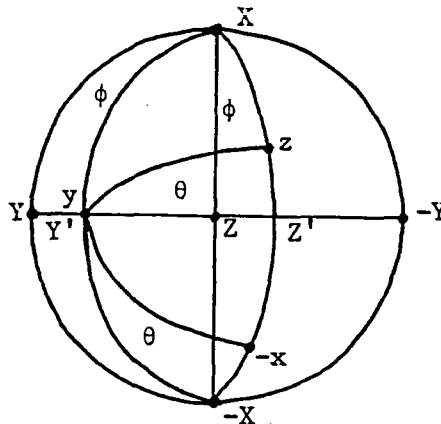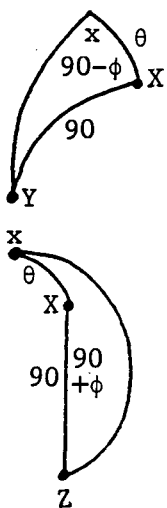The rotations are described in terms of the angles ϕ and θ as shown in Figure 39.

Figure 39. Vehicle coordinates

$$\cos\theta_{xX} = \cos\theta \tag{67}$$

$$\cos\theta_{xY} = \cos\theta \cos90 + \sin\theta \sin90 \cos(90-\phi)$$

$$= \sin\theta \sin\phi \tag{68}$$

$$\cos\theta_{xZ} = \cos\theta \cos90 + \sin\theta \sin90 \cos(90+\phi)$$
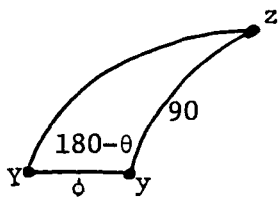
$$= -\sin\theta \sin\phi \tag{69}$$

By inspection:

$$\cos\theta_{yX} = \cos90 = 0 \tag{70}$$
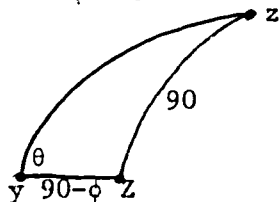
$$\cos\theta_{yY} = \cos\phi \tag{71}$$

$$\cos\theta_{yZ} = \cos(90-\phi) = \sin\phi \tag{72}$$

$$\cos\theta_{zX} = \cos(90-\theta) = \sin\theta \tag{73}$$

$$\cos\theta_{zY} = \cos\phi \cos90 + \sin\phi \sin90 \cos(180-\theta)$$

$$= -\sin\phi \cos\theta \tag{74}$$

$$\cos\theta_{zZ} = \cos90 \cos(90-\phi) + \sin90 \sin(90-\phi)\cos\theta$$

$$= \cos\phi \cos\theta \tag{75}$$

Using equations 67-75, the transformation matrix of equation 66 is given as:

$$T_2 = \begin{bmatrix} \cos\theta & \sin\theta \sin\phi & -\sin\theta \cos\phi \\ 0 & \cos\phi & \sin\phi \\ \sin\theta & -\cos\theta \sin\phi & \cos\theta \cos\phi \end{bmatrix} \qquad (76)$$

The satellite vector in the x,y,z frame is given by:

$$R_s = R_{s_x} \hat{i}_x + R_{s_y} \hat{i}_y + R_{s_z} \hat{i}_z$$

The distance from the vehicle to the satellite is:

$$\rho = \sqrt{R_{s_x}^2 + R_{s_y}^2 + (R_{s_z} - R_v)^2}$$

The direction cosines are given as:

$$\cos\theta_{x\rho} = \frac{R_{s_x}}{\rho}, \quad \cos\theta_{y\rho} = \frac{R_{s_y}}{\rho}, \quad \cos\theta_{z\rho} = \frac{(R_{s_z} - R_v)}{\rho} \qquad (77)$$

Given the satellite's ascending node, inclination, and orbit angles and the vehicle longitude, latitude, and altitude, it is possible to generate the desired direction cosines with equation 77 by performing the two satellite coordinate transformations given by equations 60 and 66.